UNIVERSITY OF CALIFORNIA
SANTA CRUZ

SYNTHESIS OF NOVEL FLUORINATED ALKOXYAMINES FOR NITROXIDE-MEDIATED PRECIPITATION POLYMERIZATION IN SUPERCRITICAL CARBON DIOXIDE

A thesis submitted in partial satisfaction
of the requirements for the degree of

MASTER OF SCIENCE

in

CHEMISTRY

by

Jennifer Marie Petraitis

March 2017

The Thesis of Jennifer M. Petraitis is approved:

_____
Professor Rebecca Braslau, Advisor

_____
Professor Bakthan Singaram, Chair

_____
Professor Joe Konopelski

_____
Tyrus Miller
Vice Provost and Dean of Graduate Studies

TABLE OF CONTENTS

List of Figures, Schemes, and Tables

Figures

Schemes

Tables

Abstract

Synthesis of Novel Fluorinated Alkoxyamines for Nitroxide-Mediated Precipitation Polymerization in Supercritical Carbon Dioxide

Jennifer M. Petraitis

Three novel fluorinated alkoxyamines were synthesized for nitroxide-mediated precipitation polymerization (NMP) of styrene in supercritical carbon dioxide. The polymerizations were conducted in supercritical carbon dioxide without excess free nitroxide to allow for a detailed study on nitroxide partitioning. The addition of a fluorinated moiety allowed for increased partitioning relative to the parent nitroxide into supercritical carbon dioxide. The loss of control over the polymerization due to nitroxide partitioning did not have a significant influence on the polymerization rate. Synthesis of polyfluorinated macroinitiators by atom transfer radical polymerization (ATRP) of fluorinated monomers was explored but thwarted due to a lack of solubility. The increased fluorine content due to polymerization of fluorinated monomers would have allowed direct control over the quantity of fluorine added to the macroinitiator and potentially influenced the quantity of nitroxide partitioning.

Acknowledgments

I would like to thank my advisor, Professor Rebecca Braslau for all of her support, patience, and confidence in me during my years at UC Santa Cruz. Rebecca's teaching style has had a big impact on me and influenced me as I have improved my teaching abilities with my own students. As a member of Rebecca's research lab, I learned how to think critically about research and gained confidence in my ability to solve problems and persevere through a challenge. My time in the Braslau lab has made me into a better chemist and student.

Thank you also to my committee members, Professor Bakthan Singaram, Professor Roger Linington, and Professor Joe Konopelski. Bakthan has given me very useful advice relating to chemistry and life during my time at UC Santa Cruz. He has always supported me and believed in my ability as a scientist, even when I didn't have faith in myself. Roger was always encouraging to me when I took his NMR class, and when he attended my second year seminar and qualifying exam. He challenged me to think outside the box which allowed me to become a better chemist. Thank you to Joe for filling in and reading my thesis once Roger left UCSC. I always enjoyed talking about chemistry with Joe during his class as well as when I was his TA. I would also like to thank Jonathan Axon for attending my qualifying exam as my outside member. The qualifying exam was one of the

biggest learning experiences of my life, and I am grateful for all I learned in positively overcoming such a challenge.

I would not have succeeded in graduate school without the support of my fellow members of the Braslau lab. I would like to acknowledge Joy Tansakul, Friederike Schaffner, Aruna Earla, Jessica Golden, Wiley Schultz-Simonton, Chad Higa, Elliot Smith, Jerin Tasnim, Longbo Li, and Malcolm Gebauer. When I first joined the lab as a summer undergraduate in 2011, I could not have asked for better mentors than Joy and Aruna. Joy and Aruna both had so much patience in teaching me and answering any questions I had. Aruna continued to be a huge support system for me during her time in the lab. As a graduate student, I entered with Chad and Elliot and I have had so many memories with both of them. Chad has become such a good friend over the years. Wiley makes me laugh on a daily basis, and in my later years I have really enjoyed getting to know Jerin and Longbo as they begin their time in the lab. Finally, Malcolm was an undergrad in the lab for only a short time, but that time gave me a friend for life.

Outside of my lab I have made great friends including Jake Haeckl, Angel Resendez, Gaby Amberchan, and Rachel Snelling. I really enjoyed my time with Jake before he went to Vancouver with Roger's group. The Singaram lab is always a fun support system, and I'm so happy to have made such good memories with them. My close friendship with Rachel is a significant reason why I have made

it to this point in grad school. I owe a lot to our farmer's market visits and coffee breaks.

Lastly, very special thanks go to my family, my parents RoseAnn and Frank Petraitis, my brother Brandon, and my boyfriend Chris Murphy. My parents have always believed in me and supported me even when I didn't believe in myself. They showed me that I was capable and deserving of success. I am so grateful for all they have given me and all the long, therapeutic phone conversations. My brother is hilarious and I could not imagine life without him. I'm grateful for him always reminding me to chill out and stop stressing so much. Of course, if it weren't for Chris I would never have attended UCSC in the first place. I'm sure that I've done my fair share to drive him insane during our mutual time in graduate school, but he has stuck with me through thick and thin. I'm grateful for all his love and support, and most importantly, patience.

Chapter 1. Introduction

1.1. Radical Polymerization Background

1.1.1. "Living" or Controlled Radical Polymerization

Radical polymerization is a well-established field of chemistry with many practical applications, however it also has several drawbacks pertaining to synthetic control. Due to the lack of mediation, monomer rapidly incorporates until the polymerization is terminated or all monomer is consumed. This results in polymer chains of varying lengths and a high polydispersity index (PDI) of 1.5 or above. In recent decades, new developments have been implemented to improve the control of traditional radical polymerizations, leading to "living" or controlled polymerizations (CRP).[1,2] A temporary radical trap is used to control the propagating radical species and minimize chain termination, as shown in Scheme 1.1.

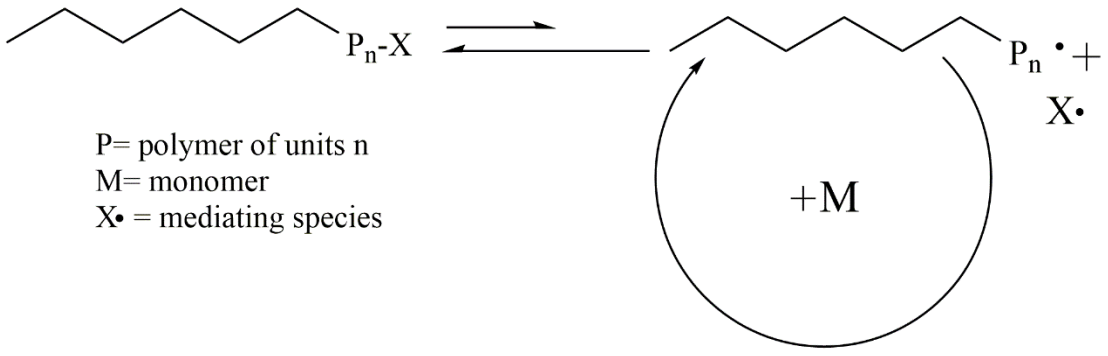

Scheme 1.1. General mechanism of controlled radical polymerization

The dormant polymer chain P_n-X is activated to the propagating species Pn• after homolytic cleavage of the bond to mediating species X•. The dormant and active

polymer chain forms are in equilibrium, favoring the dormant species. After addition of a monomer unit M, the mediating species X• reversibly traps the polymeric radical to form the dormant polymer chain. This "capping" and "uncapping" of the active polymeric radical species by the mediator allows for controlled growth of the polymer chains. It also minimizes the chances of two propagating polymer chains undergoing termination by coupling together or by disproportionation. Several varieties of controlled radical polymerizations are employed currently which differ in the types of mediating species used.

1.1.2 The Persistent Radical Effect

The persistent radical effect is the fundamental principle behind many varieties of controlled radical polymerization.[3,4] A persistent radical and a transient radical very selectively cross-couple to afford the dormant polymer chain. In the beginning stages of radical polymerizations, some transient radicals rapidly cross-couple and self-terminate. This presents an increase in concentration of persistent radicals and ensures every growing polymer chain has a mediating species to act as a cap and control the rate of polymerization. If the concentration of persistent radicals is too low, not every polymer chain is adequately monitored and growth can occur too quickly, causing high PDIs. However, if the concentration of persistent radicals is too high, transient radicals are capped too quickly and monomer addition cannot take place. The success of controlled radical polymerizations is highly dependent on the concentration and stability of the persistent radical species.

1.2 Nitroxide Mediated Radical Polymerization (NMP)

1.2.1. Common Nitroxides for NMP

Nitroxide mediated polymerization is one of the most popular methods of controlled radical polymerization.[5,6] This method makes use of a nitroxide as the mediating species between dormant and active polymer chains. Nitroxides are persistent radical species with high stability due to the resonance stabilization seen in Figure 1.1.[4]

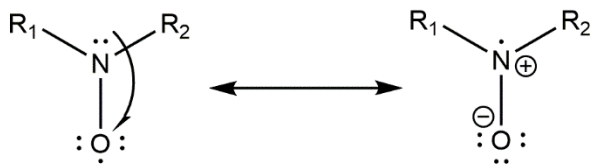

Figure 1.1 Nitroxide resonance stabilization

Three examples of nitroxides commonly employed as radical traps in NMP include 2,2,6,6-tetramethyl-1-piperidinyloxy (TEMPO),[7] *N*-*tert*-butyl-*N*-[1-diethylphosphono-(2,2-dimethylpropyl)] nitroxide (SG1),[8] and 2,2,5-trimethyl-4-phenyl-3-azahexane-3-oxy (TIPNO)[9] as seen in Figure 1.2.

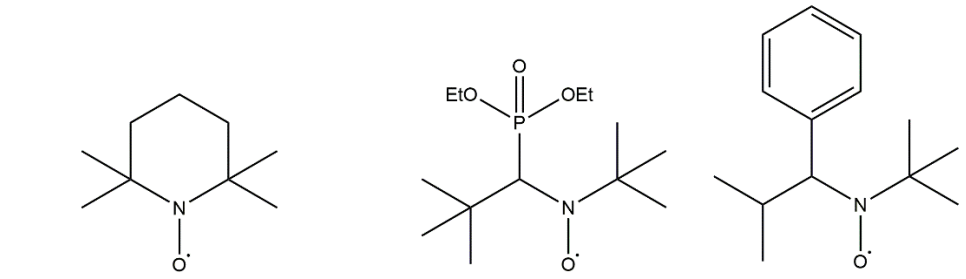

2,2,6,6-tetramethyl-1-piperidinyloxy (TEMPO)

N-tert-butyl-*N*-[1-diethylphosphono-(2,2-dimethylpropyl)] nitroxide (SG1)

2,2,5-trimethyl-4-phenyl-3-azahexane-3-oxy (TIPNO)

Figure 1.2. Examples of common nitroxides used in NMP

1.2.2. Unimolecular NMP Initiators

Hawker first introduced the use of alkoxyamines as unimolecular initiators for NMP; heating homolytically cleaves the alkoxyamine to produce a transient carbon radical species and a persistent nitroxide.[10] An example mechanism for a unimolecular system of NMP is shown in Scheme 1.2.

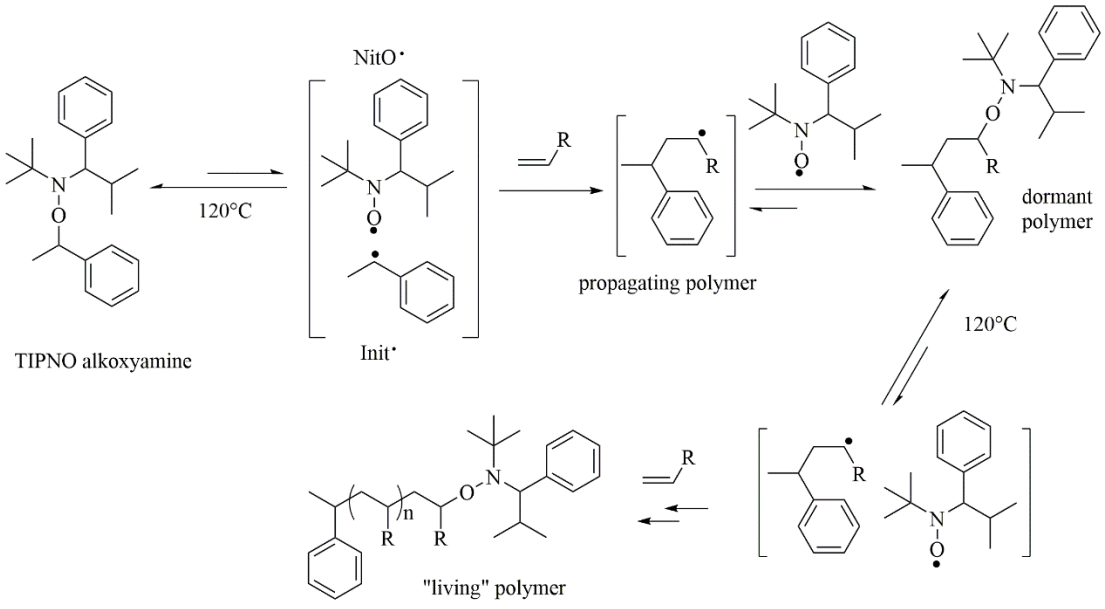

Scheme 1.2. An example of nitroxide mediated polymerization (NMP) with TIPNO

Heat cleaves the alkoxyamine homolytically to generate the initiating carbon radical species Init• and nitroxide NitO•. Polymerization is started by the addition of Init• to the monomer. Propagation of the polymer chain is monitored by the capping of NitO• to the transient carbon radical polymer to form the dormant species. Thermally uncapping the NitO• from the dormant species allows the addition of another monomer unit. Propagation continues until the heat is removed, the monomer is exhausted, or the carbon polymer radical reacts with another carbon polymer radical. Use of an alkoxyamine as a unimolecular initiation system is an effective method of NMP because the stoichiometric ratio between the transient initiating carbon species and the nitroxide cap is maintained. Nitroxide mediated polymerization yields well-defined polymers with predictable molecular weights and low PDI values.[10]

1.3. Atom Transfer Radical Polymerization (ATRP)

1.3.1. Introduction to ATRP

Atom transfer radical polymerization is another method of controlled radical polymerization, and it follows a similar mechanism to NMP. The major difference between NMP and ATRP is the capping agent. With ATRP, it is a halogen atom that gets transferred to a transition metal complex. An example of ATRP is shown in Scheme 1.3.

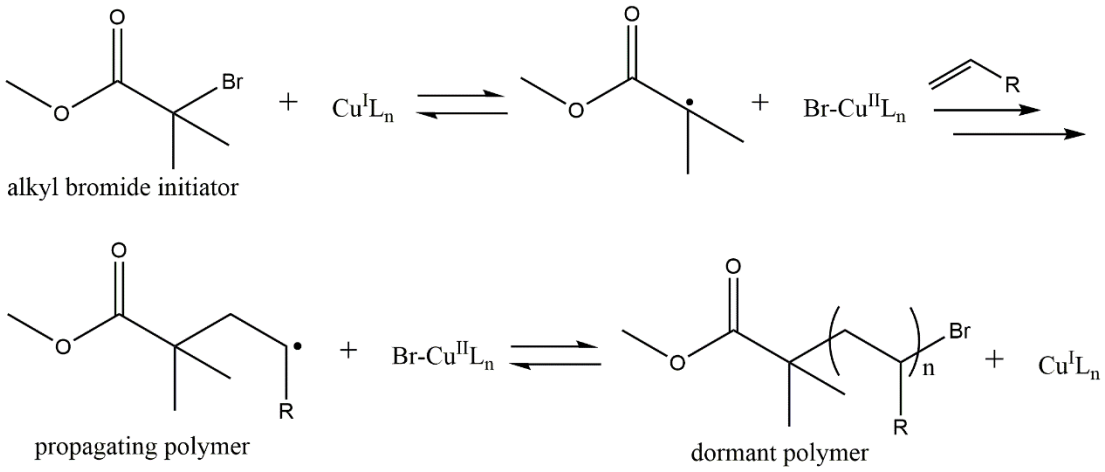

Scheme 1.3. An example of atom transfer radical polymerization (ATRP)

Copper is the most common metal used in the transition metal complex, but other metals can be used such as iron, ruthenium, and nickel.[11] A wide variety of ligands can be used such as *N,N,N',N',N''*-pentamethyldiethylenetriamine (PMDETA), 2,2'-bipyridine (bpy), or tris(2-dimethylaminoethyl)amine (Me_6TREN).[12] Upon mild heat, the copper (I) complex reacts with the alkyl bromide initiator to transfer the bromine. This results in oxidation of the copper to form a copper (II) complex. Monomer adds to the alkyl radical until it is capped by abstracting the bromine atom from the copper complex. The bromine atom is continuously transferred from the initiator to the copper complex and back, allowing for controlled propagation of the polymer chain.

1.4. Polymerizations in Supercritical Carbon Dioxide ($scCO_2$)

1.4.1. Properties of Supercritical Carbon Dioxide

One of the developments of "green chemistry" has been driven by an environmental concern to find chemically benign and environmentally friendly solvent

alternatives to the volatile organic compounds (VOC) used today.[13–15] Supercritical carbon dioxide possesses many properties that have allowed it to emerge as the most extensively used solvent alternative to traditional VOCs. Such attractive properties include low cost, low toxicity, abundance, nonflammability, and tunable solvent properties.[13,16] It can also be recycled after use to prevent contribution to greenhouse effects.

A fluid is in a supercritical state when the pressure and temperature exceed certain critical values. Increasing the temperature beyond the critical temperature (T_c) and the pressure beyond the critical pressure (P_c) allows a liquid to expand to form the supercritical state without undergoing a phase transition. Above the critical point, there is no distinct interface between the liquid and vapor phases, and one single supercritical phase exists.[17] A pressure-temperature diagram for carbon dioxide is seen in Figure 1.3.[18]

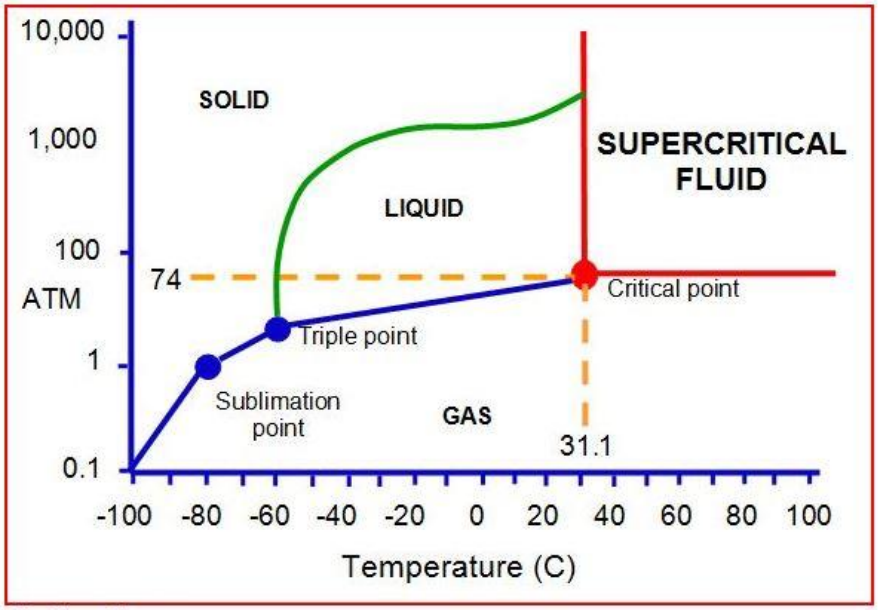

Figure 1.3. A pressure-temperature diagram for CO_2.[18]

The critical temperature for CO_2 is 31 °C and the critical pressure is 73.8 bar, making the critical point readily accessible. A supercritical fluid exhibits liquid-like densities and gas-like diffusivities. This allows for solvation of many compounds with important implications for reaction kinetics. Thus, small changes in temperature or pressure allow for tuning the solvent power. Solvent power is determined by the molecular interactions between the supercritical fluid and the solute. Increased interactions occur as the gas is compressed within the supercritical region.[13,14]

1.4.2. Supercritical CO_2 as a Solvent for Precipitation/Dispersion Polymerizations

Solubility is a very important factor in the synthesis of polymers in $scCO_2$. Both polar and nonpolar low molecular weight (MW) organic molecules are readily soluble

in $scCO_2$, but unless very high temperatures and pressures are used, high molecular weight polymers are insoluble. The only polymers that are readily soluble at high molecular weights are fluoropolymers and silicones.[19,20] For example, to dissolve a 10^5 g/mol polymer of poly(methyl methacrylate) (PMMA) in $scCO_2$, a pressure of 2000 bar and 100 °C is required.[21] Such high pressures are not practical or cost-effective for widespread implementation in polymer manufacturing.

Many varieties of controlled radical polymerizations can be performed in $scCO_2$ including NMP, ATRP, and reversible addition fragmentation chain transfer polymerization (RAFT).[22,23] When carrying out polymerizations in $scCO_2$, the system is initially a homogenous mixture of CO_2, monomer, and initiator. Since $scCO_2$ is a poor solvent for high molecular weight polymers, as the polymerization proceeds and the polymer grows in size, the monomer and initiator remain soluble in the $scCO_2$ while the polymer becomes insoluble. This makes $scCO_2$ a suitable choice for precipitation or dispersion polymerizations. Precipitation occurs at a critical degree of polymerization known as J_{crit}. After reaching J_{crit}, particles of polymer are formed as they precipitate from the continuous phase. These particles are now the main locus of polymerization. An appealing attribute of precipitation polymerizations is that the polymer product can be recovered as a powder after venting the CO_2. This avoids costly and intensive work-up procedures.

Dispersion polymerization is similar to precipitation polymerization, except colloidal stabilizers are added to prevent polymer coagulation.[24] Generally, the polymeric stabilizers used are diblock copolymers with a CO_2-philic segment

containing a siloxane or fluorocarbon and a CO_2-phobic segment to interact with the polymer particle.[13,25,26]

1.4.3. Precipitation NMP in Supercritical CO_2

Precipitation NMPs in $scCO_2$ have been performed using common nitroxides TEMPO, SG1, and TIPNO with styrene as the monomer.[27–29] Since NMP is a controlled polymerization and molecular weight growth is slow, J_{crit} can be predicted as a function of initial monomer loading using the model developed by O'Connor et al.[30] For example, at 40% (w/v) styrene, J_{crit} of 28 (M_n= 2900 g/mol) was obtained at 8% conversion. However, at 70% (w/v) styrene, J_{crit} of 114 (M_n= 11,850 g/mol) was obtained at 26% conversion.[28] It is important to note that J_{crit} is a parameter of solubility, so it is believed that a higher J_{crit} at higher initial styrene loading is due to greater polymer stability in the more monomer-rich continuous phase. The polymer is more stable amongst the unconsumed styrene monomer, so it takes longer for it to precipitate out of the $scCO_2$. The controlled/living character of the polymerization was confirmed due to narrow molecular weight distributions (PDI = 1.11-1.32). Polystyrene was recovered as a white powder after venting the CO_2.

Interestingly, Aldabbagh et al. reported in 2008 that precipitation NMP of styrene in $scCO_2$ proceeded with better control over the PDI than the corresponding solution polymerizations.[28] This was the first heterogeneous CRP to perform better than its homogenous counterpart. The increase in PDI control was achieved due to an increase in initial monomer loading of up to 70% (w/v). This high monomer loading

supports a high J_{crit} value, high solubility of the polymer in the monomer-rich continuous phase, and therefore a highly controlled PDI.

1.4.4. Nitroxide and Monomer Partitioning in $scCO_2$ Polymerizations

Polymerizations carried out without any solvent are known as bulk polymerizations. These polymerizations are homogenous because nothing precipitates away from the locus of polymerization, unlike with $scCO_2$. For homogenous NMP, the rate and degree of control is dictated by the rate at which nitroxides are able to cap and release the growing polymer chains. An example is shown in Figure 1.4. When the nitroxide is free from the polymer chain, monomer is able to add and the rate of polymerization increases. No monomer can add when nitroxide has capped the polymer, so the rate of polymerization stops. The equilibrium constant for polymerization can by determined by $K = k_d/k_a$, where k_d = rate of dissociation and k_a = rate of association.

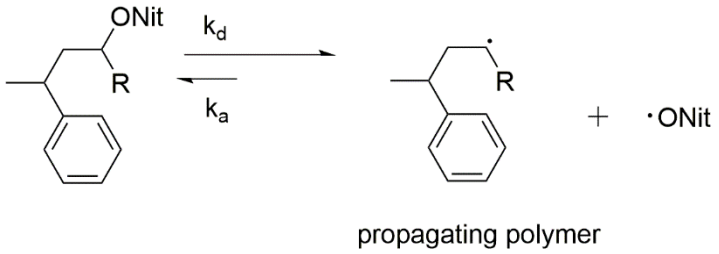

Figure 1.4. Equilibrium constant of polymerization $K = k_d/k_a$.

When comparing SG1 to TIPNO, the equilibrium constant K for SG1 is higher by a factor of 3, meaning SG1 dissociates more readily than TIPNO, since the k_a values do not vary substantially.[31] Typically, a higher propensity to dissociate corresponds to

an increase in the PDI and a decrease in control. Interestingly, in bulk, solution, and precipitation polymerizations in $scCO_2$, SG1-mediated polymerizations occur with slightly better control than the TIPNO-mediated polymerizations.[29] This effect cannot be explained using the measured rate constants from the literature and the NMP mechanism.

Precipitation polymerizations in $scCO_2$ were compared at 40% and 70% monomer loading for SG1 and TIPNO. It was found by Aldabbagh et al. that at 40% monomer loading, TIPNO gave extensive low molecular weight tailing, meaning a large number of polymer chains remained at low molecular weights. Thus, it is believed that TIPNO partitions more towards the continuous phase ($scCO_2$) or is more highly soluble in $scCO_2$ than SG1. This would cause an increase in PDI since the locus of polymerization is in the particle phase after J_{crit}.[29] The particle phase is not as controlled without a high enough concentration of nitroxide. This effect is known as nitroxide partitioning.

In contrast, monomer partitioning could increase control of the polymerization and lower the PDI. In this scenario, fewer monomer units can be added to each propagating radical after a dissociation event. This is because the monomer concentration at the locus of polymerization in the particle would be reduced. Small molecules can readily partition between the particle phase and the continuous phase because the diffusivity in $scCO_2$ has been reported to be 1-2 orders of magnitude higher than in liquids.[14] Monomer partitioning is another factor that contributes to the success of CRP in $scCO_2$ since it can result in a low PDI.

1.4.5. Precipitation ATRP in Supercritical CO_2

Limited research has been carried out in precipitation ATRP. Matyjaszewski and DeSimone were the first to report on precipitation ATRP in $scCO_2$.[32] One example precipitation ATRP polymerization is shown in Scheme 1.4. In this publication, precipitation ATRP of methyl methacrylate (MMA) was performed at 80 °C using the fluorinated ligand 4,4'-di(tridecafluoro-1,1,2,2,3,3-hexahydrononyl)-2,2'-bipyridine ($dR_{f6}bpy$) (Figure 1.5).

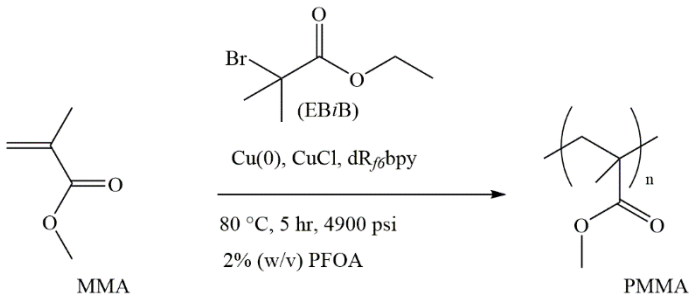

$[EBiB]_0/[Cu(0)]_0/[CuCl]_0/[dR_{f6}bpy]_0 = 1/0.5/0.5/1$

Scheme 1.4. Precipitation ATRP polymerization of MMA with polymeric stabilizer PFOA

This ligand was specifically designed to have good solubility in $scCO_2$ since fluorinated species are highly soluble. Additionally, a fluorinated polymeric stabilizer poly(1,1-dihydroperfluorooctyl acrylate) (PFOA) (Figure 1.5) was used to perform dispersion polymerizations of MMA. The polymeric stabilizer PFOA was used at low molecular weights, but the exact range of molecular weights constituting "low" was

not given. Scanning electron microscopy (SEM) analysis of particle morphology was not reported.

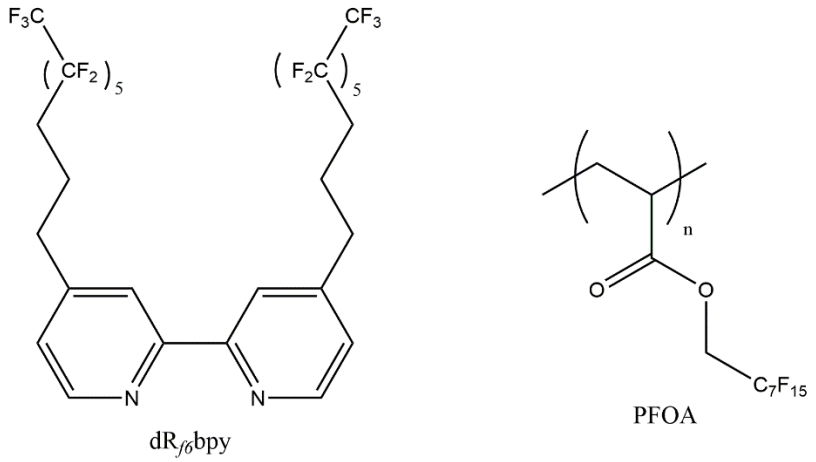

Figure 1.5. ATRP ligand $dR_{f6}bpy$ and polymeric stabilizer PFOA

A precipitation ATRP of MMA was performed by Grignard et al. with 34% (w/v) of MMA at 70 °C and 320 bar.[33] The polymerization is shown in Scheme 1.5.

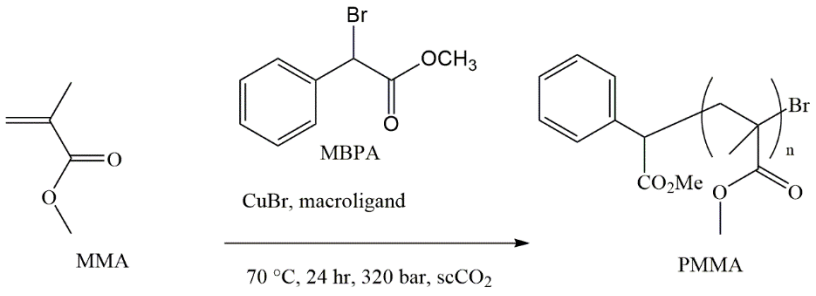

M_n of the microligand = 15,000 g/mol; 2.7 TEDETA units/chain
[MBPA]/[TEDETA] = 2; [CuBr]/[TEDETA] = 1

Scheme 1.5. Precipitation ATRP polymerization of MMA with TEDETA-based microligand in $scCO_2$

The polymerization was initiated by methyl α-bromophenylacetate (MBPA) and copper (1) bromide using an amino-based fluorinated macroligand based on *N,N,N',N'*-tetraethyldiethylenetriamine (TEDETA). The synthesis of the macroligand had been established previously by the same group,[34] and the structure of the macroligand is shown in Figure 1.6. Results were poor, with PDI = 1.90 and no distinct particle formation. The authors attributed the poor control to insufficient solubility of the ligand in $scCO_2$.

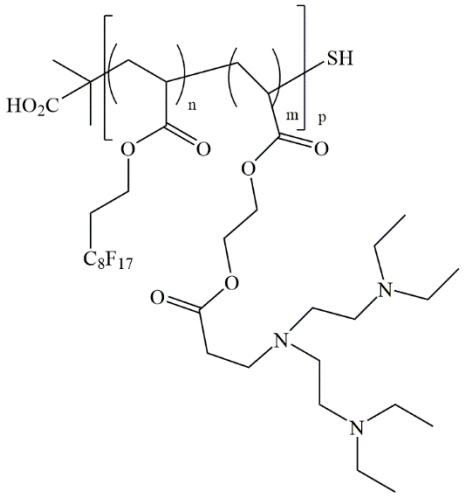

Figure 1.6. Amino-based fluorinated macroligand based on *N,N,N',N'*-tetraethyldiethylenetriamine (TEDETA).

Although Grignard suggested the lack of success of the ATRP was due to poor ligand solubility,[33] many conventional ATRP ligands are soluble in $scCO_2$, including 1,1,4,7,10,10-hexamethyltriethylenetetramine (HMTETA) and bpy.[14,35] These ligands are shown in Figure 1.7. This suggests it is not necessary to synthesize new ligands designed specifically for $scCO_2$.

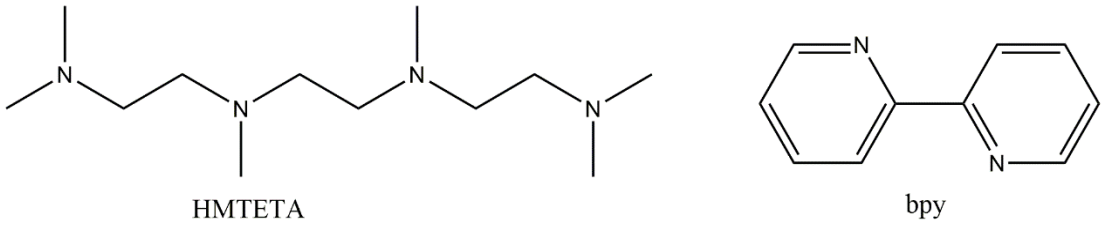

Figure 1.7. ATRP ligands HMTETA and bpy soluble in $scCO_2$

1.5. Conclusion

Controlled radical polymerization methods have been developed in recent decades to afford good control over chain lengths and PDIs. Many CRP methods are in use today, including NMP and ATRP. NMP relies on the persistent radical effect, in which a persistent radical reversibly couples with the transient radical of the growing polymer chain to generate a dormant species. Both of these CRP methods can be performed in supercritical CO_2, a "green" solvent for polymerizations that circumvents the need for VOCs. Supercritical CO_2 has many physical properties that make it an ideal supercritical fluid for polymerizations, including a readily accessible critical point. Solubility is one of the most important factors when designing $scCO_2$ polymerizations to achieve a high degree of polymerization and low PDIs. NMP studies in $scCO_2$ are currently more developed than ATRP, but the appeal of $scCO_2$ is continuing to grow due to the ease of polymer product work-up and the environmental advantages of avoiding VOCs.

While NMP in $scCO_2$ is becoming a developed field, there have been no studies reported without addition of excess free nitroxide. NMP performed in $scCO_2$ without

excess free nitroxide would allow for a direct study of nitroxide partitioning and its effect on the rate of polymerization and molecular weight distribution. Adding a fluorinated moiety to alkoxyamine initiators would potentially cause increased partitioning due to greater solubility in the continuous phase. Adjusting the amount of fluorine on the initiator could also play a role in the amount of nitroxide that partitions. Alkoxyamines with varying degrees of fluorination were designed for polymerizations in $scCO_2$.

1.6. References

(1) Otsu, T.; Yoshida, M.; Tazaki, T. *Macromol. Rapid Commun.* **1982**, *3* (2), 133.

(2) Matyjaszewski, K.; Gaynor, S.; Greszta, D.; Mardare, D.; Shigemoto, T. *J. Phys. Org. Chem.* **1995**, *8* (4), 306.

(3) Nilsen, A.; Braslau, R. *J. Polym. Sci., Part A: Polym. Chem.* **2006**, *44* (2), 697.

(4) Fischer, H. *J. Am. Chem. Soc.* **1986**, *108* (14), 3925.

(5) Darling, T. R.; Davis, T. P.; Fryd, M.; Gridnev, A. A.; Haddleton, D. M.; Ittel, S. D.; Matheson, R. R.; Moad, G.; Rizzardo, E. *J. Polym. Sci., Part A: Polym. Chem.* **2000**, *38* (10), 1706.

(6) Shipp, D. A. *J. Macromol. Sci. C.* **2005**, *45* (2), 171.

(7) Georges, M. K.; Veregin, R. P. N.; Kazmaier, P. M.; Hamer, G. K. *Macromolecules* **1993**, *26* (11), 2987.

(8) Couvreur, L.; Lefay, C.; Belleney, J.; Charleux, B.; Guerret, O.; Magnet, S. *Macromolecules* **2003**, *36* (22), 8260.

(9) Benoit, D.; Chaplinski, V.; Braslau, R.; Hawker, C. J. *J. Am. Chem. Soc.* **1999**, *121* (16), 3904.

(10) Hawker, C. J. *J. Am. Chem. Soc.* **1994**, *116* (24), 11185.

(11) Kamigaito, M.; Ando, T.; Sawamoto, M. *Chem. Rev.* **2001**, *101* (12), 3689.

(12) Matyjaszewski, K.; Xia, J. *Chem. Rev.* **2001**, *101* (9), 2921.

(13) Kendall, J. L.; Canelas, D. A.; Young, J. L.; DeSimone, J. M. *Chem. Rev.* **1999**, *99* (2), 543.

(14) Zetterlund, P. B.; Aldabbagh, F.; Okubo, M. *J. Polym. Sci., Part A: Polym. Chem.* **2009**, *47* (15), 3711.

(15) Thurecht, K. J.; Howdle, S. M. *Aust. J. Chem.* **2009**, *62* (8), 786.

(16) DeSimone, J. M.; Maury, E. E.; Menceloglu, Y. Z.; McClain, J. B.; Romack, T. J.; Combes, J. R. *Science* **1994**, *265* (5170), 356.

(17) Span, R.; Wagner, W. *J. Phys. Chem. Ref. Data* **1996**, *25* (6), 1509.

(18) http://www.novasterilis.com/index.php/application/supercritical-co2 (accessed Mar 21, 2017).

(19) Hyatt, J. A. *J. Org. Chem.* **1984**, *49* (26), 5097.

(20) Rindfleisch, F.; DiNoia, T. P.; McHugh, M. A. *J. Phys. Chem.* **1996**, *100* (38), 15581.

(21) Rindfleisch, F.; DiNoia, T.; McHugh, M. *Polym. Mater. Sci. Eng.* **1996**, *74*, 178.

(22) Barner-Kowollik, C.; Buback, M.; Charleux, B.; Coote, M. L.; Drache, M.; Fukuda, T.; Goto, A.; Klumperman, B.; Lowe, A. B.; Mcleary, J. B.; Moad, G.;

Monteiro, M. J.; Sanderson, R. D.; Tonge, M. P.; Vana, P. *J. Polym. Sci. Part Polym. Chem.* **2006**, *44* (20), 5809.

(23) Moad, G.; Rizzardo, E.; Thang, S. H. *Aust. J. Chem.* **2006**, *59* (10), 669.

(24) Kawaguchi, S.; Ito, K. In *Polymer Particles*; Okubo, M., Ed.; Springer: Berlin and Heidelberg, 2005; Vol. 175, pp 299–328.

(25) Canelas, D. A.; DeSimone, J. M. *Macromolecules* **1997**, *30* (19), 5673.

(26) Lacroix-Desmazes, P.; Andre, P.; Desimone, J. M.; Ruzette, A.-V.; Boutevin, B. *J. Polym. Sci., Part A: Polym. Chem.* **2004**, *42* (14), 3537.

(27) McHale, R.; Aldabbagh, F.; Zetterlund, P. B.; Okubo, M. *Macromol. Chem. Phys.* **2007**, *208* (16), 1813.

(28) Aldabbagh, F.; Zetterlund, P. B.; Okubo, M. *Macromolecules* **2008**, *41* (7), 2732.

(29) Aldabbagh, F.; Zetterlund, P. B.; Okubo, M. *Eur. Polym. J.* **2008**, *44* (12), 4037.

(30) O'Connor, P.; Zetterlund, P. B.; Aldabbagh, F. *Macromolecules* **2010**, *43* (2), 914.

(31) Sobek, J.; Martschke, R.; Fischer, H. *J. Am. Chem. Soc.* **2001**, *123* (12), 2849.

(32) Xia, J.; Johnson, T.; Gaynor, S. G.; Matyjaszewski, K.; DeSimone, J. *Macromolecules* **1999**, *32* (15), 4802.

(33) Grignard, B.; Jérôme, C.; Calberg, C.; Jérôme, R.; Wang, W.; Howdle, S. M.; Detrembleur, C. *Chem. Commun.* **2008**, 314.

(34) Grignard, B.; Jérôme, C.; Calberg, C.; Jérôme, R.; Detrembleur, C. *Eur. Polym. J.* **2008**, 861.

(35) Villarroya, S.; Zhou, J.; Thurecht, K. J.; Howdle, S. M. *Macromolecules* **2006**, *39* (26), 9080.

Chapter 2. Synthesis of Novel Fluorinated Alkoxyamines for Polymerizations in $scCO_2$

2.1. Introduction

Supercritical carbon dioxide ($scCO_2$) is an environmentally friendly alternative solvent to traditionally used volatile organic compounds (VOCs). It has emerged as one of the most studied VOC alternatives due to many attractive qualities such as low cost, low toxicity, abundance, nonflammability, and tunable solvent properties with minor changes to temperature and pressure.[1–3] In recent years, controlled/living polymerization studies have been conducted in $scCO_2$ with NMP and ATRP.[4–8] In this chapter, polymerizations will be reported in $scCO_2$ without excess free nitroxide, so the effect of nitroxide partitioning on control over the rate and molecular weight distribution could be studied for the first time. These studies were performed in collaboration with Dr. Fawaz Aldabbagh from the National University of Ireland, Galway and resulted in a publication in *Polymer Chemistry*.[9] Novel initiators were synthesized containing fluorinated segments on either the nitroxide or the styryl-initiating "foot" fragment of the alkoxyamine. It was hypothesized that the location of the fluorinated segment would have an effect on the degree of nitroxide partitioning, with a polyfluorinated nitroxide causing more partitioning. Since the nitroxide will contain fluorine atoms, it should partition effectively into the continuous phase, and control over the rate of polymerization and molecular weight distribution control would be expected to decline. The synthesis of the novel initiators seen in Figure 2.1 and their performance in $scCO_2$ was studied, as well as comparisons to analogous toluene solvent

polymerizations. Initiators **2.1** and **2.2** contain a fluorinated segment on the nitroxide piece (fl-NitO•), whereas **2.3** contains a fluorinated segment on the styryl "foot" (fl-foot).

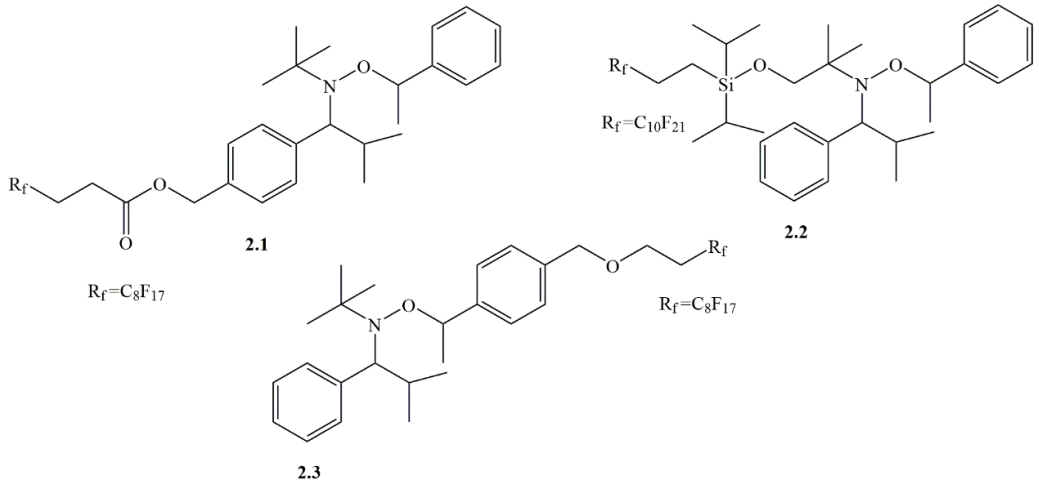

Figure 2.1. Novel alkoxyamine initiators designed for polymerizations in $scCO_2$

2.2. Synthesis of Novel fl-NitO• Initiator 2.2

The fl-NitO• initiator **2.1** was synthesized by Aruna Earla as reported in Magee et al.[9] The fl-NitO• initiator **2.2** was synthesized as shown in Scheme 2.1. Synthesis of 2-methyl-2-nitropropanol **2.4** was completed following the route of Dornow et al.[10] This alcohol was previously commercially available, but recent unavailability resulted in the discovery of the Dornow reference, which was translated from German. The synthetic steps up to the neopentyl alkoxyamine **2.9** were completed following the route of Ruehl et al.[11] The nitropropanol **2.4** was protected in high yield to form the tetrahydropyranyl ether **2.5**.

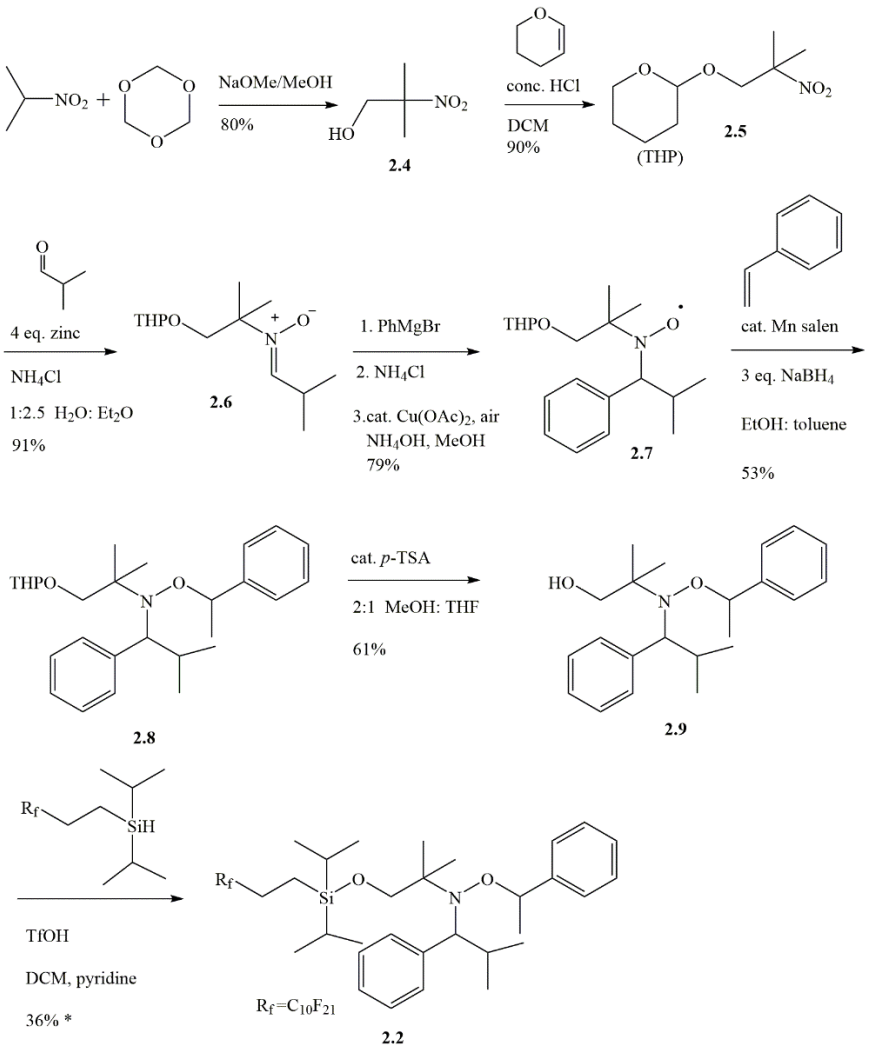

Scheme 2.1. Successful synthesis of fl-NitO• initiator **2.2**
*Reaction carried out by Aruna Earla

Next, the nitro species **2.5** was reduced with zinc powder and condensed with isobutyraldehyde to form the nitrone **2.6**. A Grignard reaction was performed followed by oxidation with air and catalytic copper (II) acetate to yield the nitroxide **2.7**. The alkoxyamine **2.8** was synthesized by coupling the nitroxide **2.7** with styrene using the manganese salen catalyst shown in Figure 2.2. The catalyst proved difficult to

synthesize, but an optimized method is described in Magee et al.[9] Recrystallization of the catalyst provided crops of colors varying from orange to brown-black. The orange crops were not properly oxidized and exhibited a clay-like texture. Only the brown-black crops can be used and have a sand-like texture. It is imperative to have a fully functional catalyst to perform the alkoxyamine synthesis. It is highly recommended that the black crop be recrystallized from H_2O to recover the most active catalyst. I was sent to Galway on our collaborative grant, and assisted the Aldabbagh group in the synthesis of alkoxyamines. The main problem was their difficulty in attaining a proper manganese salen catalyst.

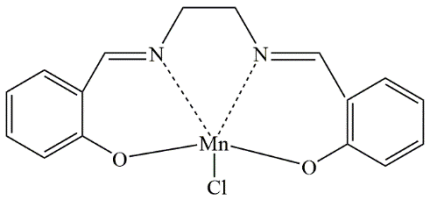

Figure 2.2. Manganese salen catalyst used to synthesize alkoxyamine **2.8**

Deprotection of the THP group on **2.8** with catalytic *p*-toluene sulfonic acid yielded the neopentyl alcohol **2.9**. The conversion of **2.9** to the final initiator **2.2** was performed following the procedure of Crich et al.[12] This reaction was attempted multiple times, but ultimately the most successful conversion was completed by Aruna Earla. This optimized procedure is described in Magee et al.[9]

2.3. Synthesis of Novel fl-foot Initiator 2.3

The synthesis of novel fl-foot initiator **2.3** is shown in Scheme 2.2.

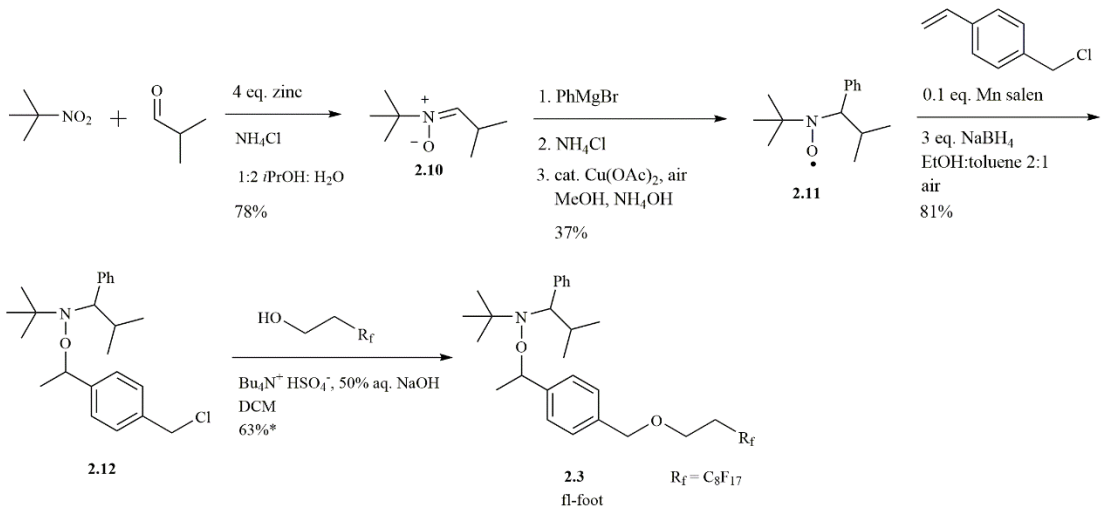

Scheme 2.2. Successful synthesis of fl-foot initiator **2.3**
*Reaction carried out by Aruna Earla

The nitrone **2.10** was synthesized following the method of O'Brien et al.[13] O'Brien's method replaced the previously used solvent mixture of 1:1 diethyl ether : water with 1:2 isopropanol : water to give enhanced yields. Next, a Grignard reaction was performed followed by oxidation with air and catalytic copper (II) acetate to yield the nitroxide **2.11**.[11] Following a modified procedure from Hawker et al., 4-vinylbenzyl chloride was coupled to the nitroxide **2.11** to form the alkoxyamine **2.12**.[14] This procedure also used the manganese salen catalyst as synthesized in Magee et al.[9] Lastly, the fl-foot alkoxyamine **2.3** was synthesized by the addition of the fluorinated alcohol 1*H*, 1*H*, 2*H*, 2*H*-perfluorodecanol with tetrabutylammonium hydrogen sulfate and 50% aqueous NaOH following the procedure of Valtola et al.[15] This procedure was attempted multiple times but ultimately optimized by Aruna Earla. This optimized procedure is described in Magee et al.[9]

2.4. Solution Polymerization Results

Solution polymerizations were performed with the three initiators **2.1**, **2.2**, and **2.3** as well as TIPNO-based alkoxyamine **2.13** and SG1-based alkoxyamine **2.14**. The solution polymerizations of styrene were performed by collaborator Christopher Magee from the Aldabbagh group in Galway, Ireland. All solution polymerizations were performed by adding the styrene (2.0 g, 19.2 mmol), alkoxyamine initiator (0.05 mmol), and toluene (1.8 mL) to a Pyrex ampoule, subjecting the mixture to several freeze-pump-thaw cycles, and sealing under vacuum. The ampoules were heated at 110 °C for various times and quenched in an ice water bath before precipitating from methanol and drying under vacuum for 24 hours. The percent conversion was measured by gravimetry.

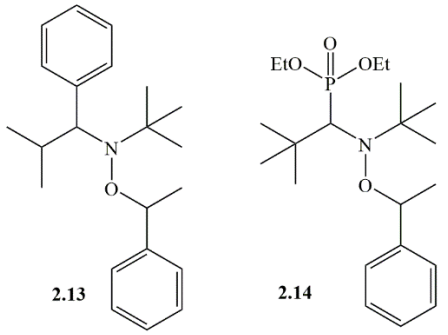

Figure 2.3. TIPNO-based and SG1-based alkoxyamine initiators

The conversion versus time plots of the solution polymerizations are shown in Figure 2.4.[9] A legend of the alkoxyamine initiators corresponding to the Figure 2.4 graph is shown in Figure 2.5. The open symbols represent the solution polymerizations

while the $scCO_2$ polymerizations are represented by the closed solid black symbols. In solution, all of the novel alkoxyamines **2.1**, **2.2**, and **2.3** gave a similar rate of polymerization to TIPNO-alkoxyamine **2.13**. This indicates that the structural modifications in the novel initiators did not have a significant effect on the equilibrium constant (K) of trapping and dissociation, and therefore there is not a significant difference on the polymerization rate. When comparing the open symbols in Figure 2.4, the upright triangle polymerized at a faster rate than the others. This symbol represents the SG1 alkoxyamine **2.14**. Since SG1 alkoxyamines generally give a faster rate of polymerization than TIPNO alkoxyamines, this result was expected.[16] Figure 2.6 (with Figure 2.5 legend) shows controlled/living character for the solution polymerizations with polydispersities (PDI, M_w/M_n) under 1.3 for most cases. Since a faster rate of polymerization frequently corresponds to a loss of control, it is reasonable that the SG1 alkoxyamine **2.14** frequently shows the highest PDI.

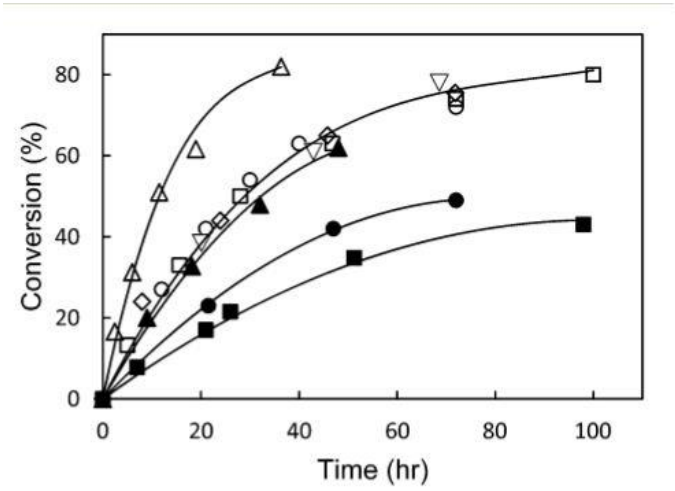

Figure 2.4.[9] Conversion versus time plots for solution (open symbols) and $scCO_2$ (closed) polymerizations. The shapes correspond to the following: fl-NitO• **2.1** = squares, fl-NitO• **2.2** = inverted triangles, fl-foot **2.3** = diamonds, TIPNO **2.13** = circles, SG1 **2.14** = triangles

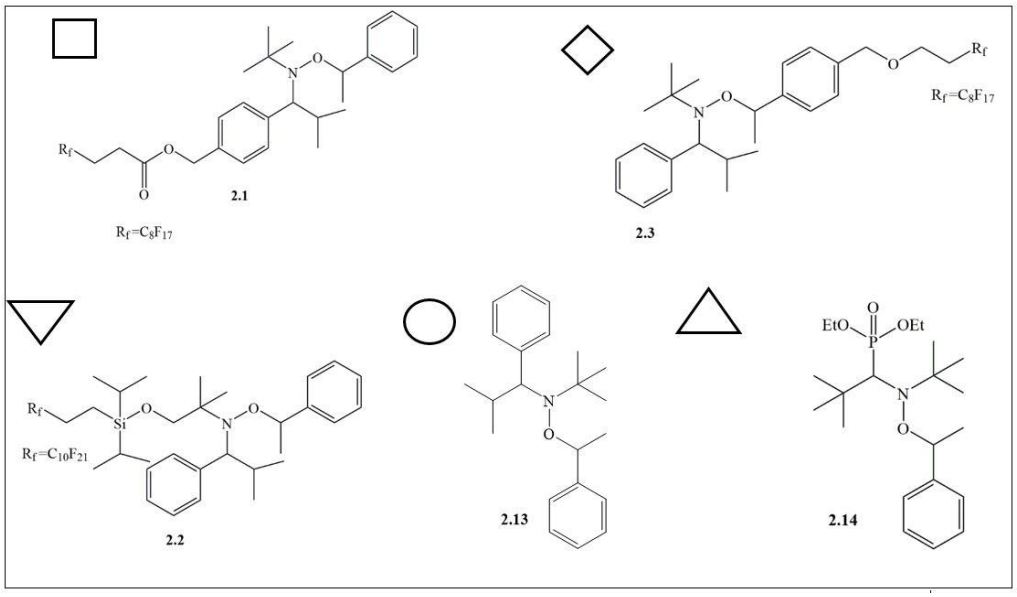

Figure 2.5. A legend of structures for Figures 2.4 and 2.6. The shapes are used for both the toluene (open) and $scCO_2$ (solid black) polymerizations.

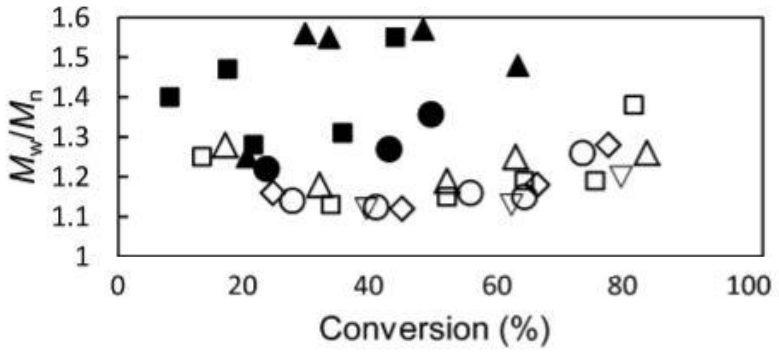

Figure 2.6.[9] Polydispersities (PDI, M_w/M_n) for solution (open) and $scCO_2$ (closed) polymerizations. The shapes correspond to the following: fl-nito **2.1** = squares, fl-nito **2.2** = inverted triangles, fl-foot **2.3** = diamonds, TIPNO **2.13** = circles, SG1 **2.14** = triangles.

2.5. Precipitation Polymerization in $scCO_2$ Results

Precipitation polymerizations of styrene in $scCO_2$ were performed with the three initiators **2.1**, **2.2**, and **2.3** as well as TIPNO-based alkoxyamine **2.13** and SG1-based alkoxyamine **2.14** by collaborator Christopher Magee from the Aldabbagh group in Galway, Ireland. The polymerizations were carried out by loading a 25 mL stainless steel Parr reactor with styrene (12.5 g, 0.12 mol), alkoxyamine (0.3125 mmol), and a magnetic stir bar. The reactor was sealed and purged for 20 minutes by bubbling CO_2 gas through the reaction mixture. Liquid CO_2 was added and the reactor was immersed in a hot oil bath. The temperature was raised to an internal temperature of 110 °C, and the pressure was controlled by addition of more liquid CO_2 until the reactor was pressurized to 30 MPa. Polymerizations were quenched by submersing the reactor in an ice water bath.[9]

Upon a critical degree of polymerization known as J_{crit}, the polymer becomes insoluble in the continuous phase and precipitates, moving the locus of polymerization from the continuous phase to the polymer phase. The precipitation polymerizations had a predicted J_{crit} value of M_n = 3,450 (8.5% conversion) following the model developed by O'Connor et al. as a function of initial monomer loading and targeted molecular weight.[17,18] Since all the precipitation polymerizations go beyond this point, they are all considered heterogeneous. As shown in Figure 2.4, SG1 alkoxyamine **2.14** (closed triangles) had a much faster rate of polymerization than the TIPNO derivatives. Figure 2.5 shows SG1 alkoxyamine **2.14** to have a higher PDI (1.25-1.57) than TIPNO alkoxyamine **2.13** (closed circles, PDI = 1.22-1.36). These results are caused by a higher K for SG1, in part due to a higher solubility of SG1 in $scCO_2$, leading to greater nitroxide partitioning away from the locus of polymerization and inferior control. It is assumed that due to SG1 containing a polar phosphonate ester in place of a phenyl group, it has less of an organic nature than TIPNO and therefore would be less likely to be in the organic polymer phase.

When comparing TIPNO alkoxyamine **2.13** (circles) to fl-NitO• alkoxyamine **2.1** (squares) in toluene (Fig. 2.4), the two alkoxyamines have a similar rate of polymerization. Surprisingly, in $scCO_2$, the rate of polymerization of TIPNO **2.13** is marginally faster. Since **2.1** contains a polyfluorinated moiety, it should be more soluble in $scCO_2$ and partition away from the locus of polymerization, leading to a faster polymerization rate. Since **2.1** does display a higher PDI (1.25-1.55) than **2.13** (1.22-1.36) (Fig. 2.5), the loss of control associated with nitroxide partitioning is

observed. This shows that nitroxide partitioning does lead to loss of control as expected, but this lack of control surprisingly has little dependence on the rate. The rate of polymerization is much more insensitive to nitroxide partitioning than expected.

Precipitation polymerizations were performed with fl-NitO• alkoxyamine **2.2** as well as fl-foot **2.3**. Fluorinated silyl nitroxide **2.2** showed less molecular weight distribution broadening compared to fluorinated ester nitroxide **2.1** (PDI = 1.29). Alkoxyamine **2.2** also surprisingly showed a slightly slower polymerization rate than TIPNO alkoxyamine **2.13**. In the case of fl-foot **2.3**, the rate of nitroxide partitioning should be comparible to TIPNO **2.13**, since the nitroxide does not contain a fluorinated segment. Fl-foot **2.3** did show a loss of control compared to TIPNO **2.13** (PDI = 1.32 versus 1.27). It has been hypothesized that the fluorine content on the propagating radical of fl-foot **2.3** leads to an increase in J_{crit} because of the increased solubility in the continuous phase. This increase in J_{crit} leads to later nucleation and a partial loss of control. It is not expected that a faster rate would lead to the observed molecular weight distribution broadening because rates and control between fl-foot **2.3** and TIPNO **2.13** were very similar in toluene solution. The data for the precipitation polymerizations of fluorinated alkoxyamines **2.2** and **2.3** compared to TIPNO are shown in Table 2.1.

Alkoxyamine	Percent Conversion	Time (hr)	M_n (molecular weight)	M_w/M_n (PDI)
fl-NitO• **2.2**	39	61	20,000	1.29
TIPNO **2.13**	42	47	17,400	1.27
fl-foot **2.3**	38	69	19,500	1.32

Table 2.1. Polymerization data for fl-NitO• **2.2** and fl-foot **2.3**. Data compared to standard TIPNO alkoxyamine **2.13** to observe changes in rate and PDI

2.6. Conclusion

Three novel alkoxyamine initiators were synthesized for NMP in $scCO_2$ and toluene solution. These three novel initiators were compared to TIPNO alkoxyamine **2.13** and SG1 alkoxyamine **2.14**. In solution, the rates were similar for all the TIPNO-based alkoxyamines, implying that the increased steric bulk of the novel initiators did not have a significant effect on the equilibrium constant *K*. The location of the fluorinated moiety on either the nitroxide or styryl foot was hypothesized to have an effect on the degree of nitroxide partitioning and therefore the rate and molecular weight distribution. The TIPNO alkoxyamines all showed superior controlled/living character to the SG1 alkoxyamine, believed to be because of the increased solubility of polar SG1 in the $scCO_2$ continuous phase compared to TIPNO derivatives. Surprisingly, while the fluorinated nitroxide alkoxyamines **2.1** and **2.2** did show a broadening of the MWD, the increased partitioning did not show an increase in polymerization rate.

It was hypothesized that the novel initiators did not contain enough fluorine atoms to exhibit a significant effect on the amount of nitroxide that partitions into

$scCO_2$ compared to TIPNO alkoxyamine. Heavily fluorinated macroinitiators would be useful to study the amount of fluorine necessary to cause a significant change in nitroxide partitioning. Attempts to prepare macroalkoxyamine initiators using ATRP of fluorinated monomers based on ATRP/NMP alkoxyamines described by Ruehl[11] et al. were thwarted due to difficulties in solubility of the components. These will be discussed in chapter 3.

2.7. References

(1) Rindfleisch, F.; DiNoia, T. P.; McHugh, M. A. *J. Phys. Chem.* **1996**, *100* (38), 15581.

(2) Kendall, J. L.; Canelas, D. A.; Young, J. L.; DeSimone, J. M. *Chem. Rev.* **1999**, *99* (2), 543.

(3) DeSimone, J. M.; Maury, E. E.; Menceloglu, Y. Z.; McClain, J. B.; Romack, T. J.; Combes, J. R. *Science* **1994**, *265* (5170), 356.

(4) Ryan, J.; Aldabbagh, F.; Zetterlund, P. B.; Okubo, M. *Polymer* **2005**, *46* (23), 9769.

(5) Aldabbagh, F.; Zetterlund, P. B.; Okubo, M. *Eur. Polym. J.* **2008**, *44* (12), 4037.

(6) McHale, R.; Aldabbagh, F.; Zetterlund, P. B.; Okubo, M. *Macromol. Rapid Commun.* **2006**, *27* (17), 1465.

(7) Xia, J.; Johnson, T.; Gaynor, S. G.; Matyjaszewski, K.; DeSimone, J. *Macromolecules* **1999**, *32* (15), 4802.

(8) Grignard, B.; Jérôme, C.; Calberg, C.; Jérôme, R.; Wang, W.; Howdle, S. M.; Detrembleur, C. *Chem Commun.* **2008**, No. 3, 314.

(9) Magee, C.; Earla, A.; Petraitis, J.; Higa, C.; Braslau, R.; Zetterlund, P. B.; Aldabbagh, F. *Polym. Chem.* **2014**, *5* (19), 5725.

(10) Dornow, A.; Müller, A. *Chem. Ber.* **1960**, *93* (1), 41.

(11) Ruehl, J.; Braslau, R. *J. Polym. Sci. Part Polym. Chem.* **2007**, *45* (10), 2015.

(12) Crich, D.; Grant, D.; Bowers, A. A. *J. Am. Chem. Soc.* **2007**, *129* (40), 12106.

(13) O'Brien, G. Ph.D. Dissertation, University of California, Santa Cruz, **2007**, p. 149.

(14) Benoit, D.; Chaplinski, V.; Braslau, R.; Hawker, C. J. *J. Am. Chem. Soc.* **1999**, *121* (16), 3904.

(15) Valtola, L.; Koponen, A.; Karesoja, M.; Hietala, S.; Laukkanen, A.; Tenhu, H.; Denifl, P. *Polymer* **2009**, *50* (14), 3103.

(16) Marque, S.; Le Mercier, C.; Tordo, P.; Fischer, H. *Macromolecules* **2000**, *33* (12), 4403.

(17) O'Connor, P.; Zetterlund, P. B.; Aldabbagh, F. *Macromolecules* **2010**, *43* (2), 914.

(18) Zetterlund, P. B. *Macromol. Theory Simul.* **2010**, *19*, 11.

Chapter 3. Attempted Synthesis of Fluorinated Macroinitiators for Polymerizations in $scCO_2$

3.1. Introduction

Previous NMP polymerizations performed with novel fluorinated initiators in $scCO_2$ did not exhibit a significant nitroxide partitioning effect.[1] It was hypothesized that the fl-foot initiator **2.3** would show more nitroxide partitioning and therefore an increase in polymerization rate and a broader molecular weight distribution compared to the other derivatives. However, there was little difference in rate between the fl-foot **2.3** and fl-nitroxide **2.1** and **2.2** initiators, and only a slight broadening of the molecular weight distribution when comparing the fluorinated derivatives to TIPNO. Plus, the fl-foot and fl-nitroxide initiators polymerized at a slower rate than the TIPNO-based alkoxyamine, but enhanced nitroxide partitioning should suggest a faster rate. Thus, the rate of polymerization appears to be insensitive to the amount of nitroxide partitioning.

Because of these surprising results, it was suggested that the previous fl-foot and fl-nitroxide initiators did not contain enough fluorine atoms to cause a significant shift in the quantity of nitroxide that would partition compared to the parent TIPNO nitroxide. Thus, fluorinated macroinitiators **3.1** and **3.2** containing significant amounts of fluorine became a target of synthesis to see if the increased quantity of fluorine causes a difference in nitroxide partitioning behavior. Polymerization of the fluorinated acrylate monomer 1*H*,1*H*,2*H*,2*H*-perfluorodecyl acrylate **3.3** would allow large

numbers of fluorine atoms to be added to a macroinitiator. The two ATRP-NMP bidirectional macroinitiators **3.1** and **3.2** were modified from initiators previously designed by Hill[2] et al. and Ruehl[3] et al., using ATRP to incorporate the fluorinated acrylate monomer for polymerization studies in $scCO_2$. It was planned to perform three polymerizations with each macroinitiator to provide a range of fluorine incorporation in order to study the amount of fluorine necessary to cause significant nitroxide partitioning. The syntheses of the precursor alkoxyamines were successful until the polymerization step. Polymerization conditions that allow full solubility and thus reactivity of the monomer were never found.

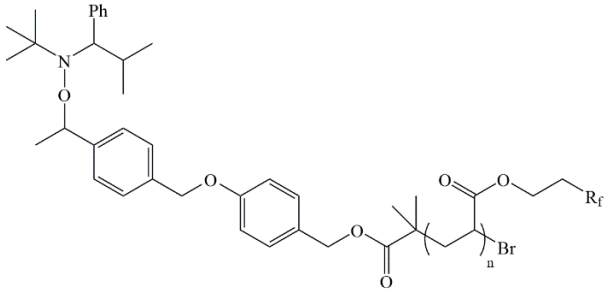

3.1

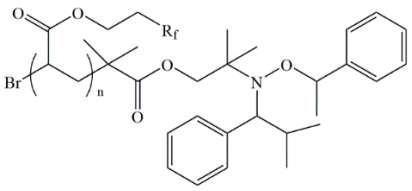

3.2

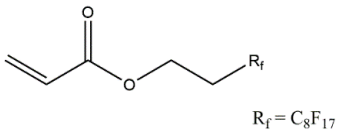

3.3

Figure 3.1. Structures of fl-foot macroinitiator **3.1,** fl-nitroxide macroinitiator **3.2,** and fluorinated monomer **3.3**

3.2. Synthesis of Precursor to fl-foot Macroinitiator 3.1

Routes to both macroinitiators consisted of two parts: synthesis of the small molecule alkoxyamine ATRP initiators; and the attempted polymerization step. The successful small molecule steps for the fl-foot macroinitiator were accomplished following routes by O'Brien[4] et al. and Hill[2] et al. The synthesis of nitrone **2.10** was accomplished following the O'Brien procedure in which the solvent system 1:2 *i*PrOH: H_2O lead to high yields.

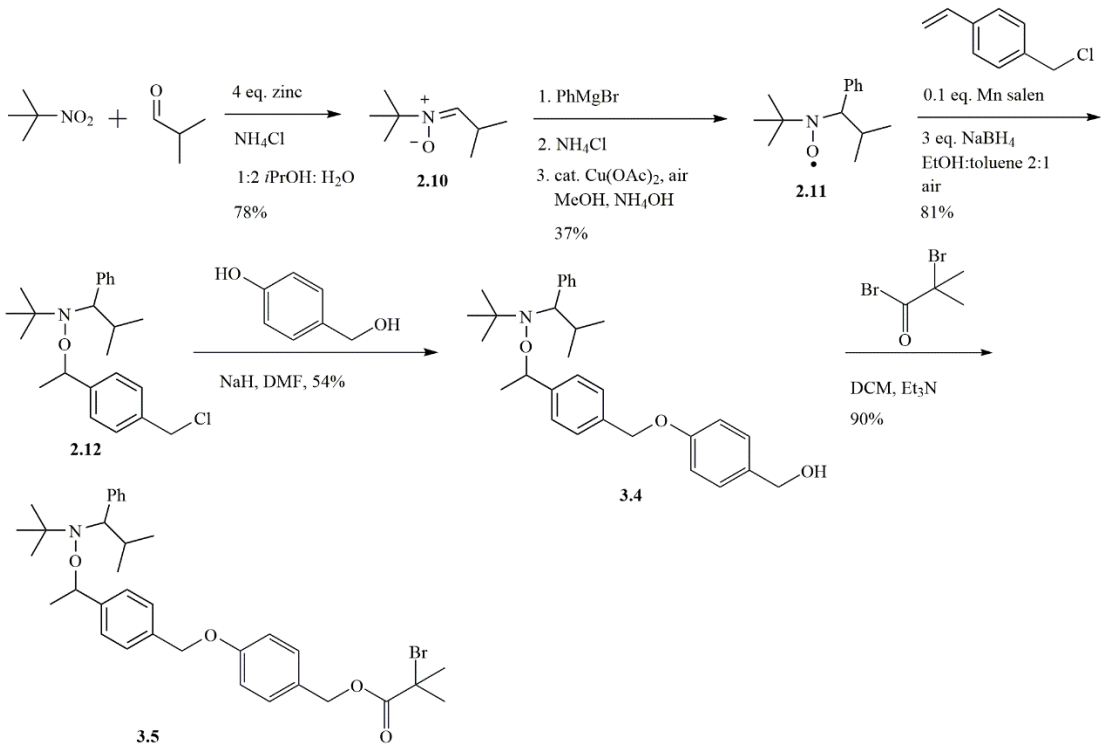

Scheme 3.1. Small molecule synthetic steps of ATRP initiator towards preparation of fl-foot macroinitiator **3.1**

The synthetic route through chlorinated alkoxyamine **2.12** was described in chapter 2. The formation of **3.4** was completed by performing an S_N2 reaction on the chlorinated

alkoxyamine **2.12** following the procedure of Hill[2] et al. Next, novel bidirectional ATRP initiator **3.5** was prepared by reaction of 2-bromo-2-methylpropionyl bromide with alcohol **3.4** under anhydrous conditions. This step was modified from that described by Ruehl[3] et al. It was found that the 2-bromo-2-methylpropionyl bromide and triethylamine needed to be freshly vacuum distilled before use and the dichloromethane required drying over calcium hydride. This reaction was successful only when care was taken to ensure all reagents were purified and anhydrous. Successful polymerization of fluorinated monomer **3.3** with initiator **3.5** would have afforded the desired polyfluorous macroinitiator **3.1**.

3.3. Synthesis of Precursor to fl-nitroxide Macroinitiator 3.2

The successful synthesis of the small molecule precursors to fl-nitroxide macroinitiator **3.2** were completed following the routes of Dornow[5] et al. and Ruehl[3] et al. The 2-methyl-2-nitropropanol **2.4** was synthesized following the Dornow method once **2.4** was no longer commercially available.

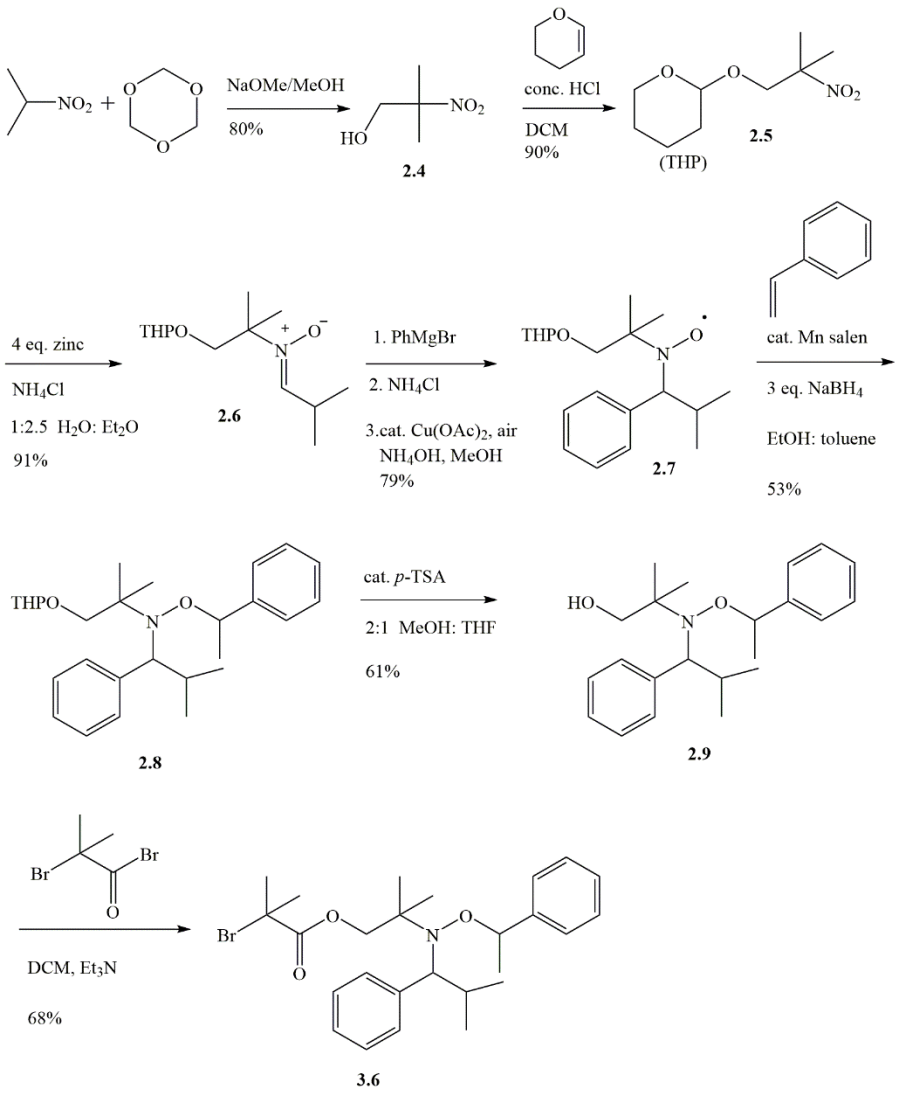

Scheme 3.2. Synthetic steps of small molecule precursors to prepare fl-nitroxide macroinitiator **3.2**

The synthetic steps up to neopentyl alcohol alkoxyamine **2.9** were repeated from chapter 2. The formation of ATRP-NMP initiator **3.6** was carried out by reaction of alcohol **2.9** under anhydrous conditions with 2-bromo-2-methylpropionyl bromide and triethylamine in dichloromethane. This step was modified from Ruehl[3] et al., and

proved more difficult than anticipated. Previously, Ruehl dried the dichloromethane over calcium hydride but did not distill the other two components. It was found that the reaction was successful when the triethylamine and 2-bromo-2-methylpropionyl bromide were both freshly vacuum distilled, along with drying the solvent. Successful polymerization of fluorinated monomer **3.3** with initiator **3.6** would have yielded the final macroinitiator **3.2**.

3.4 Polymerization Attempts

The most difficult aspect of the ATRP polymerization was ensuring solubility of all the components of the polymerization. The fluorinated monomer **3.3** was not able to readily solubilize the copper catalyst nor the ligand. This meant the polymerizations could not be performed in bulk; solvent would be required to solubilize all the components. All polymerizations were performed no hotter than 80 °C in order to prevent accidental thermal activation of NMP. All polymerization reaction mixtures were freeze-pump-thawed to remove oxygen and run for 24 hours. Since the correct polymerization conditions needed to be determined, a model initiator ethyl 2-bromo-2-methylpropanoate **3.7** was used so as not to waste the precious initiators **3.1** and **3.2**. A general polymerization using the commercial model initiator is shown in Scheme 3.3.

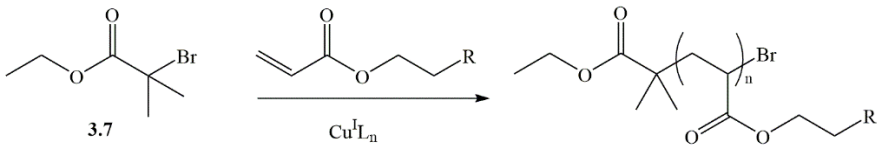

Scheme 3.3. Polymerization using model initiator **3.7**

The model initiator **3.7** was used for practice to find the correct conditions to allow for adequate solubility of all components. *n*-Butyl acrylate was sometimes used in place of the fluorinated monomer to conserve the fluorinated monomer. Table 3.1 shows the polymerizations attempted with the model initiator **3.7**.

Entry	Initiator	Monomer	Metal Species and Ligand	Solvent	Results
1	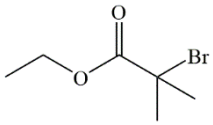 **3.7**	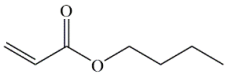 (*n*-butyl acrylate)	Copper (I) chloride 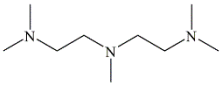 (PMDETA)	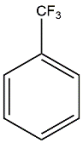 (TFT)	No conversion
2	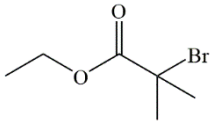 **3.7**	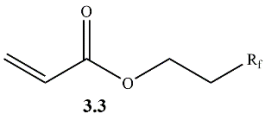 **3.3** $R_f = C_8F_{17}$	Copper (I) bromide 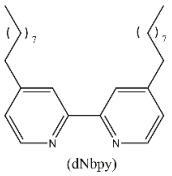 (dNbpy)	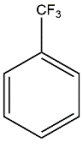 (TFT)	**41% conversion**
3	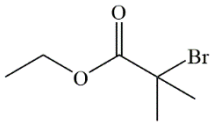 **3.7**	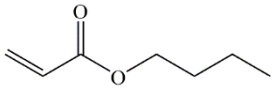 (*n*-butyl acrylate)	Copper (I) bromide 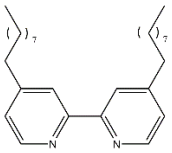 (dNbpy)	none	Solid Obtained
4	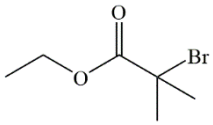 **3.7**	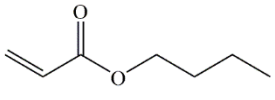 (*n*-butyl acrylate)	Copper (I) bromide 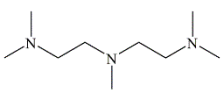 (PMDETA)	none	Solid Obtained

Table 3.1. Polymerization attempts with model initiator **3.7**

Entry 1 shows a polymerization attempted with *n*-butyl acrylate under classic ATRP conditions. The only change was the incorporation of trifluorotoluene (TFT) as solvent. This was added to practice running polymerizations that weren't done in bulk. The classic conditions were not successful. Next, Entry 2 shows a successful polymerization with the fluorinated monomer **3.3** with a change in Cu source and ligand to 4,4′-dinonyl-2,2′-dipyridyl (dNbpy). This ligand has been successfully used in ATRP polymerizations with fluorinated monomer.[6] Changing the copper source between copper (I) chloride and copper (I) bromide has no effect on the polymerization. Polymerizations have been performed successfully with both copper sources. Entry 3 showed that these same conditions worked without the TFT, however the components were clearly insoluble throughout the process; adding the solvent achieved better polymerization results. Lastly, it was shown that PMDETA was a usable ligand in Entry 4, so PMDETA could potentially be used with fluorinated monomers.

Next, polymerizations using the conditions from Entry 2 were attempted with initiators **3.5** and **3.6**. The majority of the polymerizations were attempted with **3.5** because it is a novel compound and therefore is more interesting. Polymerizations were attempted with ligands PMDETA as well as dNbpy. Attempts were also made with and without solvent. Entries 2 and 6 in Table 3.2 used the same conditions as the successful polymerization with the model initiator (Entry 2) in Table 3.1. However, this previously successful set of conditions did not work using **3.5** and **3.6**. It is unknown why these conditions failed. Perhaps the polymerization kinetics are slower with **3.5** and **3.6** compared to the model. For both attempts with results in bold in Table 3.2 (Entries 2

and 6), all reagents were initially soluble, however no polymer was observed. A model polymerization using a precursor to the novel macroinitiator **3.1** is shown in Scheme 3.4. It was proposed to run three polymerizations with **3.5** and **3.6** to synthesize a total of six macroinitiator samples with varying fluorine amounts. In order to circumvent solubility difficulties, fluorinated monomer **3.3** would be polymerized with *n*-butyl acrylate in three ratios: 1:1 *n*-butyl acrylate: **3.3**, 1:4 *n*-butyl acrylate: **3.3**, and 4:1 *n*-butyl acrylate: **3.3**. All polymerizations would be performed with 150 equivalents of monomer.

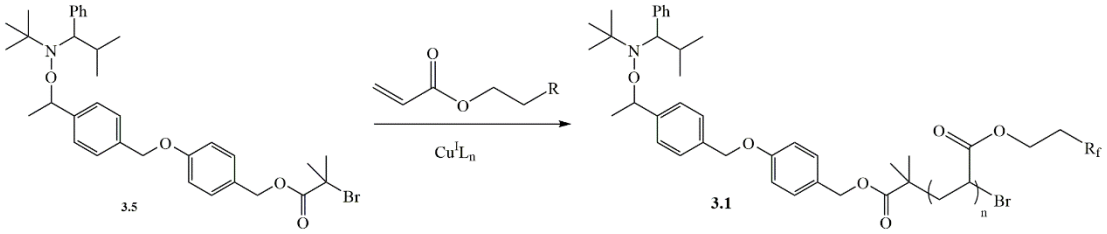

Scheme 3.4. Example ATRP polymerization with precursor **3.5**

Entry	Initiator	Monomer	Metal Species and Ligand	Solvent	Results
1	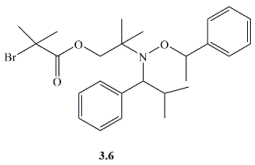 3.6	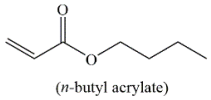 (*n*-butyl acrylate)	Copper (I) chloride 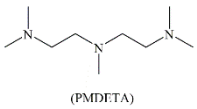 (PMDETA)	None	No conversion
2	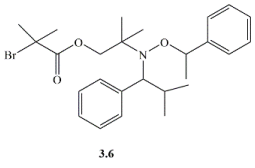 3.6	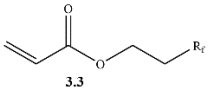 3.3 $R_f = C_8F_{17}$	Copper (I) bromide 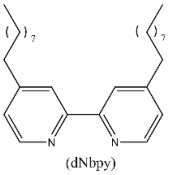 (dNbpy)	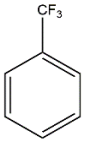 (TFT)	**No conversion**

3	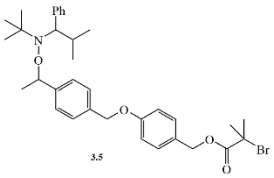	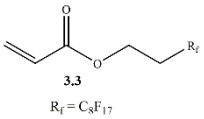	Copper (I) chloride 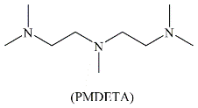	None	No conversion
4	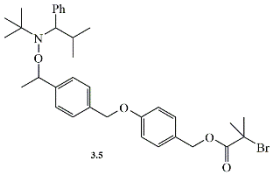	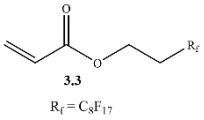	Copper (I) bromide 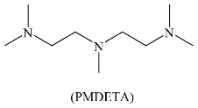	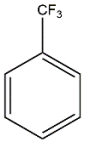	No conversion
5	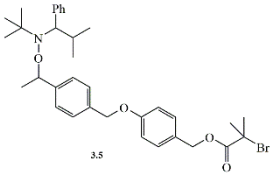	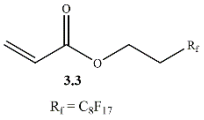	Copper (I) bromide 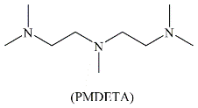	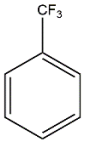	No conversion
6	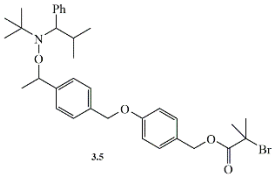	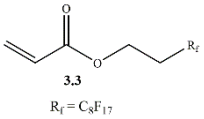	Copper (I) bromide 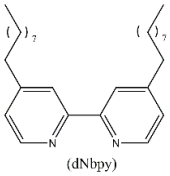	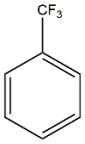	**No conversion**
7	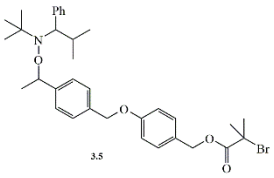	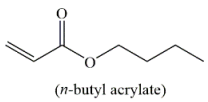	Copper (I) bromide 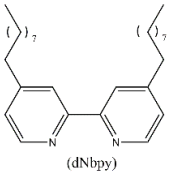	None	No conversion

Table 3.2. Polymerization attempts with initiators **3.5** and **3.6**

3.5. Conclusion

The ATRP-NMP bidirectional initiators **3.5** and **3.6** were synthesized, but polymerization to afford the highly fluorinated macroinitiators **3.1** and **3.2** were not successful. Initial difficulties following the Ruehl[3] synthetic route to afford the ATRP initiators were resolved. It is unknown why the polymerizations did not work with **3.5** and **3.6**. Since the polymerizations could not be performed, further studies could not be conducted to examine the effect of increased quantities of fluorine on nitroxide partitioning in $scCO_2$.

3.6. References

(1) Magee, C.; Earla, A.; Petraitis, J.; Higa, C.; Braslau, R.; Zetterlund, P. B.; Aldabbagh, F. *Polym. Chem.* **2014**, *5* (19), 5725.

(2) Hill, N. L.; Braslau, R. *J. Polym. Sci., Part A: Polym. Chem.* **2007**, *45* (11), 2341.

(3) Ruehl, J.; Braslau, R. *J. Polym. Sci., Part A: Polym. Chem.* **2007**, *45* (10), 2015.

(4) O'Brien, G. Ph.D. Dissertation, University of California, Santa Cruz, **2007,** p. 149.

(5) Dornow, A.; Müller, A. *Chem. Ber.* **1960**, *93* (1), 41.

(6) Alaimo, D.; Beigbeder, A.; Dubois, P.; Broze, G.; Jérôme, C.; Grignard, B. *Polym. Chem.* **2014**, *5* (18), 5273.

Chapter 4. Experimental

4.1 Materials

Triethylamine (Fisher, >99%) was distilled under reduced pressure prior to use. 2-Bromo-2-methylpropionyl bromide (Acros, 98%) was distilled under reduced pressure prior to use. Tetrahydrofuran (THF) (Fisher Scientific) was dried over sodium/benzophenone (Fisher Scientific) when anhydrous conditions were required. Dichloromethane (Fisher Scientific) was dried over calcium hydride (Fisher Scientific) when anhydrous conditions were required. Water was deionized. All other chemicals were used as received. Manganese salen catalyst was prepared following the procedure of Magee et al.[1] Analytical TLC was performed using commercial Whatman plates coated with silica gel (0.25 mm). *Para*-anisaldehyde (PAA) TLC stain was made from a mixture of ethanol (37.5 mL), concentrated sulfuric acid (2.00 mL), glacial acetic acid (0.43 mL), and *p*-anisaldehyde (2.5 mL). Flash chromatography was performed on Sorbent Technologies Silica Gel Standard Grade 60Å.

4.2 Instrumentation

NMR spectra were collected in $CDCl_3$ at ambient temperature on a Varian 500 MHz spectrometer unless otherwise noted. The spectra were recorded with $CHCl_3$ peak (δ= 7.27) as internal standard for ^{1}H-NMR and $CDCl_3$ triplet (δ= 77.27) for ^{13}C-NMR. FTIR spectra were recorded neat on a Perkin-Elmer spectrometer. HRMS was recorded on a benchtop Mariner electrospray ionization time-of-flight (ESITOF) mass spectrometer.

4.3 Synthetic Procedures

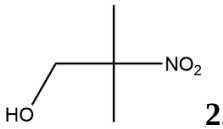

2.4

Preparation of 2-methyl-2-nitropropanol[2] 2.4

Following the procedure of Dornow et al.,[2] sodium methoxide (20 mg, 0.37 mmol) was transferred to a round-bottom flask with 70 µL of methanol and stirred at room temperature. 2-Nitropropane (8.639 g, 96.97 mmol) was added, and the reaction mixture was heated gently by waving a heat gun at the flask for 15-20 seconds. Paraformaldehyde (3.058 g, 101.8 mmol) was added in 10 portions over 5 minutes. A second portion of sodium methoxide (7.5 mg, 0.14 mmol) was added with 30 µL of MeOH, and the flask was stirred at 90 °C in an oil bath for 15 minutes. The reaction mixture was cooled to room temperature and diluted with 200 mL of $CHCl_3$, then washed with 15 mL of 10% HCl, 15 mL of water, and 15 mL of brine. The solution was dried over $MgSO_4$, filtered, and concentrated to yield a white solid (7.97 g, 79.7% yield).

TLC: 1:1 hexanes/ethyl acetate, UV, *p*-anisaldehyde stain, R_f = 0.64.

mp: 84-87 °C (lit mp = 86-89 °C).

^{1}H-NMR (500 MHz, $CDCl_3$): δ 3.88 (s, 2H), 2.18 (br s, 1H), 1.61 (s, 6H).

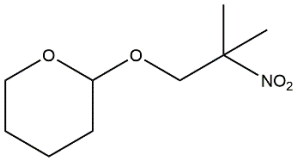

2.5

Preparation of 2-(2-methyl-2-nitropropoxy)oxane[3] 2.5

Following the procedure of Ruehl et al.,[3] 2-methyl-2-nitropropanol (7.80 g, 65.5 mmol), 3,4-dihydro-2*H*-pyran (5.78 g, 68.8 mmol) and 55 mL of CH_2Cl_2 were added to a round-bottom flask and stirred open to air. Once the reactants dissolved to form a clear solution, 0.7 mL of concentrated HCl was added dropwise. The reaction mixture was stirred at room temperature open to air overnight. The next day, 135 mL of water was added. The organic layer was separated, and the aqueous layer was extracted with CH_2Cl_2 (3 x 15 mL). The organic layers were combined, washed with 15 mL of brine, dried over $MgSO_4$, filtered, and concentrated to yield a brown oil (12.1 g, 90.1% yield).

TLC: 80:20 hexanes/ethyl acetate, UV, *p*-anisaldehyde stain, R_f = 0.35.

^{1}H-NMR (500 MHz, $CDCl_3$): δ 4.63 (t, *J* = 3.0 Hz, 1H), 3.99 and 3.72 (AB spin system, *J* = 10.4 Hz, 2H), 3.79-3.75 and 3.55-3.52 (two m, 1H each), 1.79-1.50 (m, 6H), 1.64 (s, 3H), 1.60 (s, 3H).

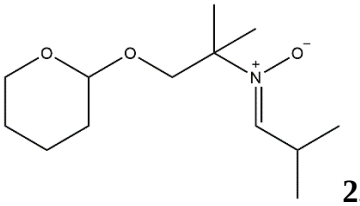

2.6

Preparation of *N*-[1,1-Dimethyl-2-(tetrahydro-pyran-2-yloxy)-ethyl]-*N*-isobutyl-nitrone[3] 2.6

Nitro compound **2.5** (12.1 g, 59.4 mmol), isobutyraldehyde (8.57 g, 119 mmol), ammonium chloride (3.50 g, 65.4 mmol), 50 mL of diethyl ether, and 122 mL of water were added to a round-bottom flask. The flask was cooled to 0 °C, and zinc powder (15.5 g, 238 mmol) was added in portions over 5 minutes. The flask was allowed to warm to room temperature and stirred for 40 hours open to air. The reaction mixture was filtered through Celite® and rinsed with 40 mL of MeOH. The organic layer was separated, and the aqueous layer was extracted with CH_2Cl_2 (3 x 20 mL). The organic layers were combined, washed with 15 mL of brine, dried over $MgSO_4$, filtered, and concentrated to yield a yellow oil (13.1 g, 90.9% yield).

TLC: 75:25 ethyl acetate/methanol, UV, *p*-anisaldehyde stain, R_f = 0.66.

^{1}H-NMR (500 MHz, $CDCl_3$): δ 6.66 (d, *J* = 7.0 Hz, 1H), 4.60 (dd, *J* = 3.3, 3.8 Hz, 1H), 3.85- 3.80 and 3.55-3.50 (two m, 1H each), 3.75 and 3.72 (AB spin system, *J* =10 Hz, 2H), 3.24-3.19 (m, 1H), 1.77-1.45 (m, 6H), 1.51 (s, 3H), 1.46 (s, 3H), 1.12 (d, *J*= 7 Hz, 3H), 1.11 (d, *J*= 7 Hz, 3H).

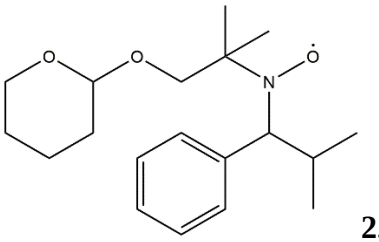

2.7

Preparation of *N*-[1,1-dimethyl-2-(tetrahydro-pyran-2-yloxy)-ethyl]-*N*-(2-methyl-1-phenyl-propyl)-nitroxide[3] 2.7

All glassware was flame-dried and cooled under nitrogen prior to use. All needles were oven-dried prior to use. Nitrone **2.6** (4.00 g, 16.4 mmol) and 29 mL of THF were added via syringe to a round-bottom flask under nitrogen. The flask was cooled to 0 °C, and phenylmagnesium bromide (1.0 M in ether, 33 mL, 33 mmol) was added drop-wise via syringe. The reaction was stirred at room temperature overnight, then quenched with 20 mL of saturated NH_4Cl and 20 mL of water at 0 °C. The organic layer was separated, and the aqueous layer was extracted with CH_2Cl_2 (3 x 15 mL). The organic layers were combined, dried over $MgSO_4$, filtered, and concentrated to yield a yellow oil as the crude hydroxylamine. Methanol (96 mL), aqueous NH_4OH (14.5 M, 3.3 mL), and copper acetate (0.15 g, 0.82 mmol) were added, and air was bubbled through the reaction mixture for 30 minutes. The solution changed from yellow to green in color in 2 minutes. The reaction mixture was concentrated and partitioned between 50 mL of $CHCl_3$, 50 mL of water, and 20 mL of saturated aqueous Na_2SO_4. The organic layer was separated, and the aqueous layer was extracted with $CHCl_3$ (3 x 15 mL). The organic layers were combined, washed with 20 mL of saturated aqueous $NaHSO_4$, dried over $MgSO_4$, filtered, and concentrated to yield a bright orange oil. This crude nitroxide

was purified by flash chromatography using 80:20 hexanes/ethyl acetate as the eluent to yield an orange oil as a mixture of diastereomers (4.14 g, 78.7% yield).

TLC: 80:20 hexanes/ethyl acetate, UV, *p*-anisaldehyde stain, R_f = 0.57.

^{1}H-NMR (500 MHz, $CDCl_3$, mixture of diastereomers, with phenylhydrazine): δ 7.44-6.84 (m, 10H), 4.51 and 4.05 (two m, 1H each), 3.76 and 3.44 (two m, 2H each), 3.64 and 3.44 (AB spin system, *J*= 8 Hz, 2H each), 3.29 and 3.17 (two d, *J*= 10 Hz, 1H each), 2.34 and 1.53 (two m, 1H each), 1.87-1.38 (two m, 6H each), 1.27, 1.15, 0.87, 0.69 (four s, 3H each), 1.15, 1.14, 0.59, 0.58 (four d, *J*= 4 Hz, 3H each).

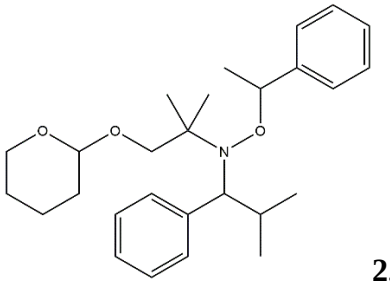

2.8

Preparation of *N*-[1,1-dimethyl-2-(tetrahydro-pyran-2-yloxy)-ethyl]-*N*-(2-methyl-1-phenyl-propyl)-*O*-(1-phenyl-ethyl)-hydroxyamine[3] 2.8

Nitroxide **2.7** (4.00 g, 12.5 mmol), styrene (2.60 g, 25.0 mmol), Mn(salen) catalyst (0.89 g, 0.50 mmol), sodium borohydride (1.42 g, 37.5 mmol), 44 mL of toluene, and 70 mL of EtOH were added to a round-bottom flask. Air was bubbled through the reaction mixture for 10 minutes, then the air bubbler was removed and the flask stirred open to air overnight. The reaction mixture changed from brown to black in color. The

crude mixture was concentrated and partitioned between 100 mL of CH_2Cl_2 and 150 mL of water. The organic layer was separated, and the aqueous layer was extracted with CH_2Cl_2 (4 x 20 mL). The organic layers were combined, dried over $MgSO_4$, and concentrated to yield a dark brown mixture of product and catalyst (3.76 g). The crude mixture was purified via flash chromatography using 60:40 CH_2Cl_2/hexanes as the eluent to yield a brown oil as a mixture of diastereomers (2.81 g, 52.9% yield).

TLC: 60:40 CH_2Cl_2/hexanes, UV, *p*-anisaldehyde stain, R_f = 0.48.

^{1}H-NMR (500 MHz, $CDCl_3$, mixture of diastereomers): δ 7.5-7.2 (m, 20H), 5.14-5.07 (two m, 1H each), 4.59, 4.55, 4.27, 4.12 (four t, *J*= 3.5 Hz, 1H each), 3.93-3.31 (m, 2H each), 3.26, 3.22, 2.86, 2.83 (four d, *J*= 10 Hz, 1H each), 2.35 and 1.45 (two m, 1H each), 1.91-1.40 (m, 12H), 1.69, 1.60 (two d, *J*= 6.0 Hz, 3H each), 1.31, 0.75, 0.63, 0.22 (four d, *J*= 6.5 Hz, 3H each), 1.26, 1.18, 1.13, 1.02 (four s, 3H each).

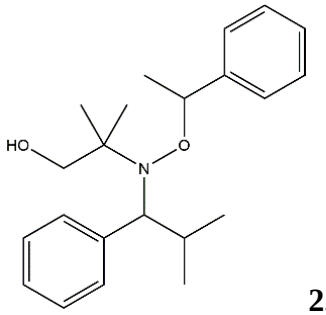

2.9

Preparation of 2-methyl-2-[(2-methyl-1-phenyl-propyl)-(1-phenyl-ethoxy)-amino]-propan-1-ol[3] 2.9

THP-protected alkoxyamine **2.8** (2.81 g, 6.61 mmol), *p*-toluenesulfonic acid (0.114 g, 0.661 mmol), 112 mL of MeOH, and 60 mL of THF were added to a round-bottom flask. The mixture was stirred overnight, after which the mixture was neutralized by adding enough $NaHCO_3$ to raise the pH to 7. After refrigeration for 24 hours, the solids were removed by filtration and the solution was concentrated to yield a colorless oil as a mixture of two diastereomers (1.37 g, 60.8% yield).

TLC: 80:20 hexanes/ethyl acetate, UV, *p*-anisaldehyde stain, R_f= 0.52.

^{1}H-NMR (500 MHz, $CDCl_3$, mixture of two diastereomers): δ 7.5-7.2 (m, 20H), 4.93 and 4.90 (two q, *J*= 7 Hz, 1H each), 3.65, 3.40, 3.21, 3.14 (four d in 2 AB spin systems, *J*= 11 Hz, 2H each), 2.95 and 2.65 (two d, *J*= 10.5 Hz, 1H each), 2.45 and 1.45 (two m, 1H each), 1.67 and 1.59 (two d, *J*= 7 Hz, 3H each), 1.36, 0.87, 0.60, and 0.24 (four d, *J*= 6.5 Hz, 3H each), 1.29, 1.12, 0.70, and 0.43 (four s, 3H each).

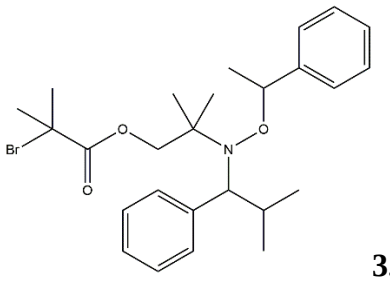

3.6

Preparation of 2-methyl-2-[(2-methyl-1-phenylpropyl)(1-phenylethoxy)amino]propyl 2-bromo-2-methylpropanoate[3] 3.6

All glassware was flame-dried and cooled under nitrogen prior to use. Following the procedure of Ruehl et al.,[3] triethylamine and 2-bromo-2-methylpropionyl bromide were distilled under reduced pressure prior to use. Alkoxyamine **2.9** (0.250 g, 0.733 mmol) was diluted with 5 mL of dry CH_2Cl_2 and transferred to a round bottom flask and stirred at 0 °C under nitrogen. Triethylamine (0.31 mL, 2.2 mmol) was diluted with 2 mL of dry CH_2Cl_2 and added slowly to the reaction flask. The reaction mixture was stirred overnight for 21 hours under nitrogen and gradually allowed to warm to room temperature. The reaction mixture changed in color from colorless to brown. The reaction mixture was washed with water (4 x 30 mL), dried over Na_2SO_4, filtered, and concentrated to yield 850 mg of brown solid. The crude product was purified by flash chromatography using 95:5 hexanes/ethyl acetate as the eluent to yield a colorless oil as a mixture of diastereomers (242 mg, 68.2%).

TLC: 95:5 hexanes/ethyl acetate, UV, *p*-anisaldehyde stain, R_f= 0.43.

^{1}H-NMR (500 MHz, $CDCl_3$): δ 7.48-7.19 (m, 20H), 4.99 and 4.95 (two q, *J*= 6.5 Hz, 1H each), 4.19, 4.01, 3.59, and 3.53 (four d, *J*= 11 Hz, 1H each), 3.43 and 3.33 (two d, *J*= 10.5 Hz, 1H each), 2.40 and 1.47 (two m, 1H each), 2.01 and 1.94 (two s, 3H each), 1.66 and 1.58 (two d, *J*= 6.5 Hz, 3H each), 1.37, 0.99, 0.58, and 0.26 (four d, *J*= 6 Hz, 3H each), 1.27, 1.07, 0.84, and 0.59 (four s, 3H each).

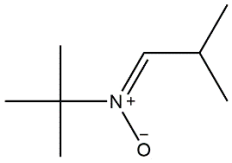

2.10

Preparation of *N*-tert-butyl-*α*-isopropyl nitrone[4] 2.10

Following the procedure of O'Brien,[4] 2-methyl-2-nitropropane (5.00 g, 48.5 mmol), isobutyraldehyde (6.99 g, 97.0 mmol), ammonium chloride (2.86 g, 53.4 mmol), and 1:2 isopropanol : water (20:40 mL) were added to a round-bottom flask and stirred at 0 °C. Zinc powder (12.68 g, 194.0 mmol) was added portion-wise over 20 minutes, and the reaction mixture was stirred overnight open to air and allowed to warm to room temperature. The reaction mixture was filtered through Celite® and washed with 100 mL of CH_2Cl_2 and 30 mL of water. The organic layer was separated, and the aqueous layer was extracted with CH_2Cl_2 (3 x 20 mL). The organic layers were combined, dried over $MgSO_4$, filtered, and concentrated to yield a colorless oil (5.43 g, 78.1% yield).

TLC: 90:10 $CHCl_3$/MeOH, UV, R_f= 0.55.

^{1}H-NMR (500 MHz, $CDCl_3$): δ 6.60 (d, *J*= 7 Hz, 1H), 3.11 (m, 1H), 1.43 (s, 9H), 1.06 (d, *J*= 7 Hz, 6H).

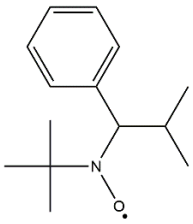

2.11

Preparation of 2,2,5-Trimethyl-4-phenyl-3-azahexane-3-nitroxide[3] 2.11

All glassware was flame-dried and cooled under nitrogen prior to use. Nitrone **2.10** (2.84 g, 19.8 mmol) and 22 mL of THF were added to a 2-neck round-bottom flask and stirred at 0 °C. Phenylmagnesium bromide (1.0 M, 39.7 mL, 39.7 mmol) was added drop-wise. The reaction flask was allowed to warm to room temperature and stirred overnight for 21 hours. The reaction mixture was quenched with 10 mL of saturated NH_4Cl and 30 mL of water. The organic layer was separated, and the aqueous layer was extracted with CH_2Cl_2 (4 x 15 mL). The organic layers were combined, washed with 10 mL of brine, dried over $MgSO_4$, filtered, and concentrated to yield 2.84 g of orange oil as the crude hydroxylamine. Methanol (86 mL), aqueous NH_4OH (14.5 M, 7 mL), and copper acetate (180 mg, 1.00 mmol) were added, and the flask was bubbled with air for 20 minutes. The reaction mixture was orange after 18 minutes, so 5 mg additional copper acetate was added to the flask. The flask was bubbled with air for ten additional minutes and the color changed from orange to dark green. The reaction

mixture was concentrated and partitioned between 70 mL of $CHCl_3$, 70 mL of water, and 30 mL of saturated $NaHSO_4$. The layers were separated, and the aqueous layer was extracted with $CHCl_3$ (3 x 15 mL). The organic layers were combined, washed with 30 mL of saturated $NaHSO_4$, dried over $MgSO_4$, filtered, and concentrated to yield 1.98 g of bright orange oil as the crude nitroxide. The nitroxide was purified by flash chromatography using 95:5 hexanes/ethyl acetate as the eluent to yield an orange oil (1.60 g, 36.7% yield).

TLC: 95:5 hexanes/ethyl acetate, UV, *p*-anisaldehyde stain, R_f = 0.53.

^{1}H-NMR: (500 MHz, $CDCl_3$, with phenylhydrazine): δ 7.44-7.16 (m, 5H), 3.45 (d, *J*= 6.5 Hz, 1H), 2.33 (m, 1H), 1.27 (s, 9H), 1.15 and 0.58 (two d, *J*= 7 Hz, 6H).

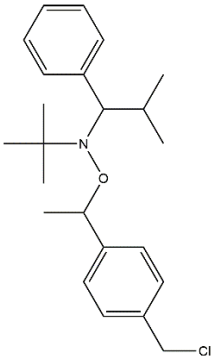

2.12

Preparation of 1-(4'-chloromethylphenyl)-1-(2',2',6',6'-tetramethyl-1-piperidinyloxy)ethyl alkoxyamine[5] 2.12

Following a modified procedure of Hawker et al.,[5] nitroxide **2.11** (1.20 g, 5.44 mmol), 4-vinylbenzyl chloride (1.66 g, 10.9 mmol), Mn(salen) catalyst (0.59 g, 1.6 mmol),

sodium borohydride (0.62 g, 16 mmol), 20 mL of toluene, and 28 mL of EtOH were added to a round-bottom flask and stirred at room temperature. The reaction mixture was bubbled with air for five minutes and the color changed from orange to dark brown. The air bubbler was removed and the reaction mixture was stirred at room temperature overnight. The next morning, volatiles were removed in vacuo, and the residue was partitioned between 40 mL of water and 40 mL of hexanes. The organic layer was separated, and the aqueous layer was extracted with hexanes (3 x 15 mL). The organic layers were combined, washed with 10 mL of $NaHCO_3$, washed with 10 mL of brine, dried over $MgSO_4$, filtered, and concentrated to yield 2.37 g of a dark brown oil. The crude alkoxyamine was purified by flash chromatography using 10:1 hexanes/CH_2Cl_2 as the eluent to yield a colorless oil as a mixture of diastereomers (1.66 g, 81.4% yield).

TLC: 10:1 hexanes/CH_2Cl_2, UV, *p*-anisaldehyde stain, R_f= 0.48.

^{1}H-NMR: (500 MHz, $CDCl_3$, mixture of diastereomers): δ 7.45-7.17 (m, 18H), 4.92 (m, 1H), 4.62 and 4.59 (two s, 2H each), 3.44 and 3.33 (two d, *J*= 10.5 Hz, 1H each), 2.33 (m, 1H), 1.64 and 1.56 (two d, *J*= 7 Hz, 3H each), 1.32, 0.94, 0.58, and 0.24 (four d, *J*= 6 Hz, 3H each), 1.06 and 0.79 (two s, 9H each).

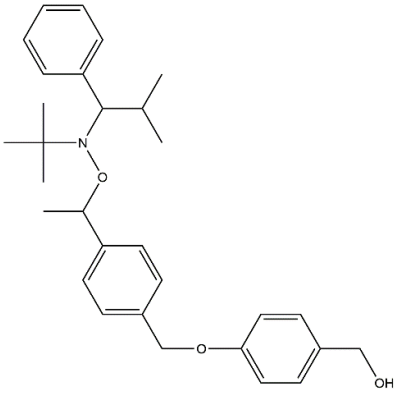

3.4

Preparation of [4-(4-{1-[*N*-tert-butyl-*N*-(2-methyl-1-phenyl-propyl)-aminooxy]-ethyl}-benzyloxy)-phenyl]-methanol[6] 3.4

Following the procedure of Hill et al.,[6] all glassware was flame-dried prior to use. 4-Hydroxymethyl phenol (0.37 g, 2.9 mmol) was dissolved in 110 mL of DMF and added to a round-bottom flask and stirred at 0 °C under nitrogen. Sodium hydride (0.160 g, 4.01 mmol) was added and the reaction mixture stirred for one hour at room temperature. Alkoxyamine **2.12** was dissolved in 10 mL of DMF and added to the reaction mixture, and stirred at room temperature overnight for 22 hours under nitrogen. The reaction mixture was partitioned between 30 mL of CH_2Cl_2 and 50 mL of water. The layers were separated, and the organic layer was washed with water (4 x 20 mL) and brine (3 x 10 mL). The organic layer was dried over $MgSO_4$, filtered, and concentrated to yield 1.06 g of an orange oil. The product was purified by flash chromatography using 4:1 hexanes/ethyl acetate as the eluent to yield a light yellow oil as a mixture of diastereomers (0.80 g, 54% yield).

TLC: 4:1 hexanes/ethyl acetate, UV, *p*-anisaldehyde stain, R_f= 0.33.

^{1}H-NMR: (500 MHz, $CDCl_3$, mixture of diastereomers): δ 7.45-6.97 (m, 26H), 5.10 and 5.04 (two s, 2H each), 4.93 (m, 1H), 4.62 (d, *J*= 5 Hz, 2H), 3.46 and 3.33 (two d, *J*= 10 Hz, 1H each), 2.33 (m, 1H), 1.88 (s, 1H), 1.63 and 1.54 (two d, *J*= 6.5 Hz, 3H each), 1.30, 0.91, 0.54, and 0.21 (four d, *J*= 6.5 Hz, 3H each), 1.05 and 0.80 (two s, 9H each).

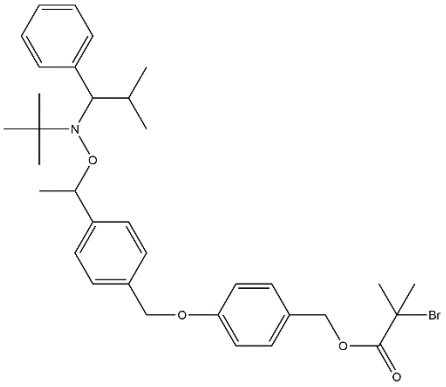

3.5

Preparation of [4-(1-{[tert-butyl(2-methyl-1-phenylpropyl)amino]oxy}ethyl)phenyl]methyl] 2-bromo-2-methylpropanoate[3] **3.5**

Following a modified procedure of Ruehl et al.,[3] all glassware was flame-dried and cooled under nitrogen prior to use. Triethylamine was distilled under reduced pressure. Dichloromethane was dried over calcium hydride. 2-Bromo-2-methylpropionyl bromide was distilled under reduced pressure. The alkoxyamine **3.4** (0.378 g, 0.820 mmol) was dissolved in 1 mL of dry CH_2Cl_2 and transferred to a round bottom flask stirring at 0 °C under nitrogen. Triethylamine (0.35 mL, 2.5 mmol) was dissolved in 2

mL of dry CH_2Cl_2 and transferred to the round bottom flask. 2-Bromo-2-methylpropionyl bromide (0.20 mL, 1.6 mmol) was dissolved in 9 mL of dry CH_2Cl_2 and added drop-wise to the reaction mixture. The flask was stirred overnight under nitrogen and gradually allowed to warm to room temperature. After 24 hours, the reaction mixture was washed with water (4 x 20 mL). The aqueous layers were extracted with CH_2Cl_2 (2 x 15 mL). The organic layers were combined, washed with 10 mL of brine, dried over $MgSO_4$, filtered, and concentrated to yield 1.53 g of brown oil. The product was purified by flash column chromatography with 100% CH_2Cl_2 as the eluent to yield a light yellow oil as a mixture of diastereomers (0.452 g, 90.4% yield).

TLC: 4:1 hexanes/ethyl acetate, UV, *p*-anisaldehyde stain, R_f= 0.34.

^{1}H-NMR: (500 MHz, $CDCl_3$, mixture of diastereomers): δ 7.46-6.97 (m, 26H), 5.14 (two d, *J*= 4 Hz, 2H each), 5.09 and 5.03 (two s, 2H each), 4.93 (two m, 1H each), 3.43 and 3.31 (two d, *J*= 9.5 Hz, 1H each), 2.34 (two m, 1H each), 1.93 and 1.92 (two s, 3H each), 1.63 and 1.55 (two d, *J*= 6.5 Hz, 3H each), 1.30, 0.91, 0.55 and 0.22 (four d, *J*= 6 Hz, 3H each), 1.04 and 0.70 (two s, 9H each).

^{13}C-NMR: (125 MHz, $CDCl_3$, DEPT, mixture of diastereomers): δ 171.55, 158.96, 145.70 (CH), 144.89 (CH), 142.42 (CH), 142.25 (CH), 135.80 (CH), 135.05 (CH), 130.92 (CH_3), 129.84 (CH_3), 127.42 (CH), 127.22 (CH), 126.45 (CH), 126.22 (CH), 115.00 (CH), 114.92 (CH), 83.27 (CH), 82.46 (CH), 77.22 (CH), 70.06 (CH_3), 67.51

(CH_3), 60.58 (CH_2), 55.89 (CH_2), 32.08 (CH_3), 31.74 (CH_3), 28.46 (CH_3), 28.31(CH_3), 24.78 (CH_2), 23.24 (CH_2), 22.18 (CH_3), 22.01 (CH_3), 21.21 (CH_3).

FTIR: 3057, 2973, 1734, 1613, 1514, 1462, 1387, 1272, 1156, 1107, 1010, 825, 702 cm^{-1}.

HRMS: mass calcd for $C_{34}H_{45}BrNO_4$ $[M+H]^+$: 610.2532, found 610.2507.

4.4 References

(1) Magee, C.; Earla, A.; Petraitis, J.; Higa, C.; Braslau, R.; Zetterlund, P. B.; Aldabbagh, F. *Polym. Chem.* **2014**, *5* (19), 5725.

(2) Dornow, A.; Müller, A. *Chem. Ber.* **1960**, *93* (1), 41.

(3) Ruehl, J.; Braslau, R. *J. Polym. Sci., Part A: Polym. Chem.* **2007**, *45* (10), 2015.

(4) O'Brien, G.; Ph.D. Dissertation, University of California, Santa Cruz, **2007**, p. 149.

(5) Dao, J.; Benoit, D.; Hawker, C. J. *J. Polym. Sci., Part A: Polym. Chem.* **1998**, *36* (12), 2161.

(6) Hill, N. L.; Braslau, R. *J. Polym. Sci., Part A: Polym. Chem.* **2007**, *45* (11), 2341.

Appendix

^{1}H NMR, ^{13}C NMR, IR data

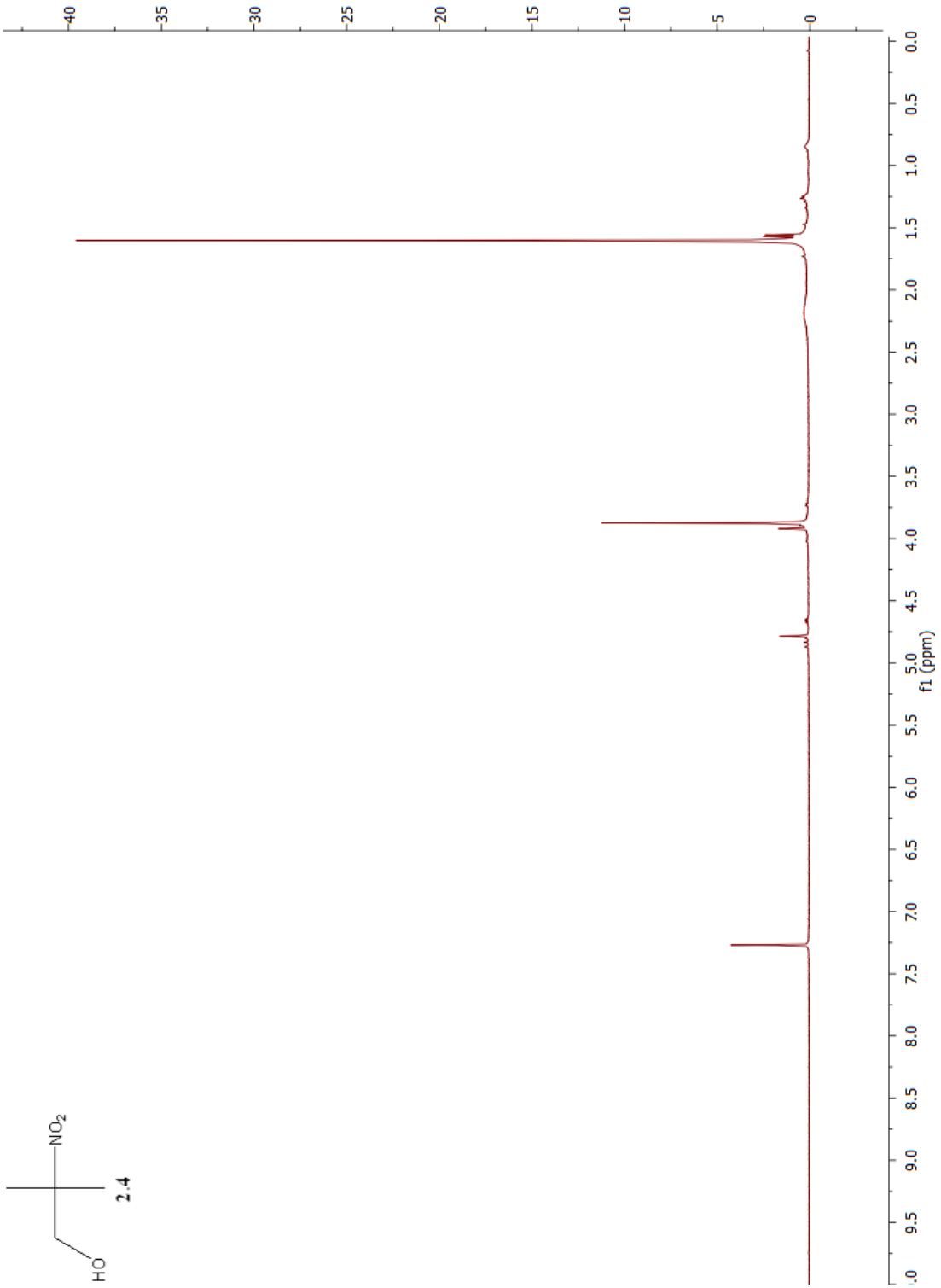
NO2
HO
2.4
f1 (ppm)

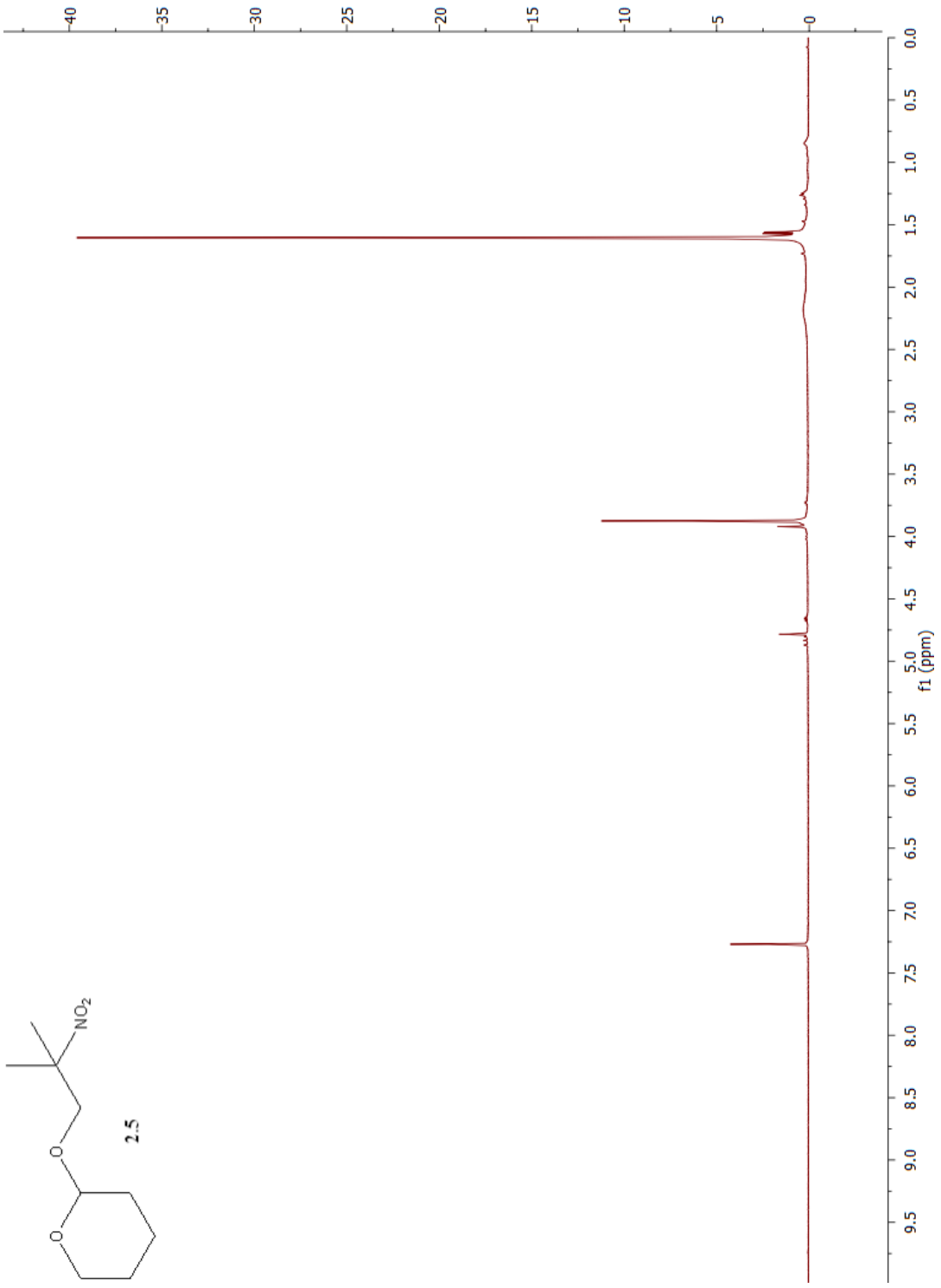
NO2
O
O
2.5
40
35
30
25
20
15
10
5
0
0.0
0.5
1.0
1.5
2.0
2.5
3.0
3.5
4.0
4.5
5.0
5.5
6.0
6.5
7.0
7.5
8.0
8.5
9.0
9.5
f1 (ppm)

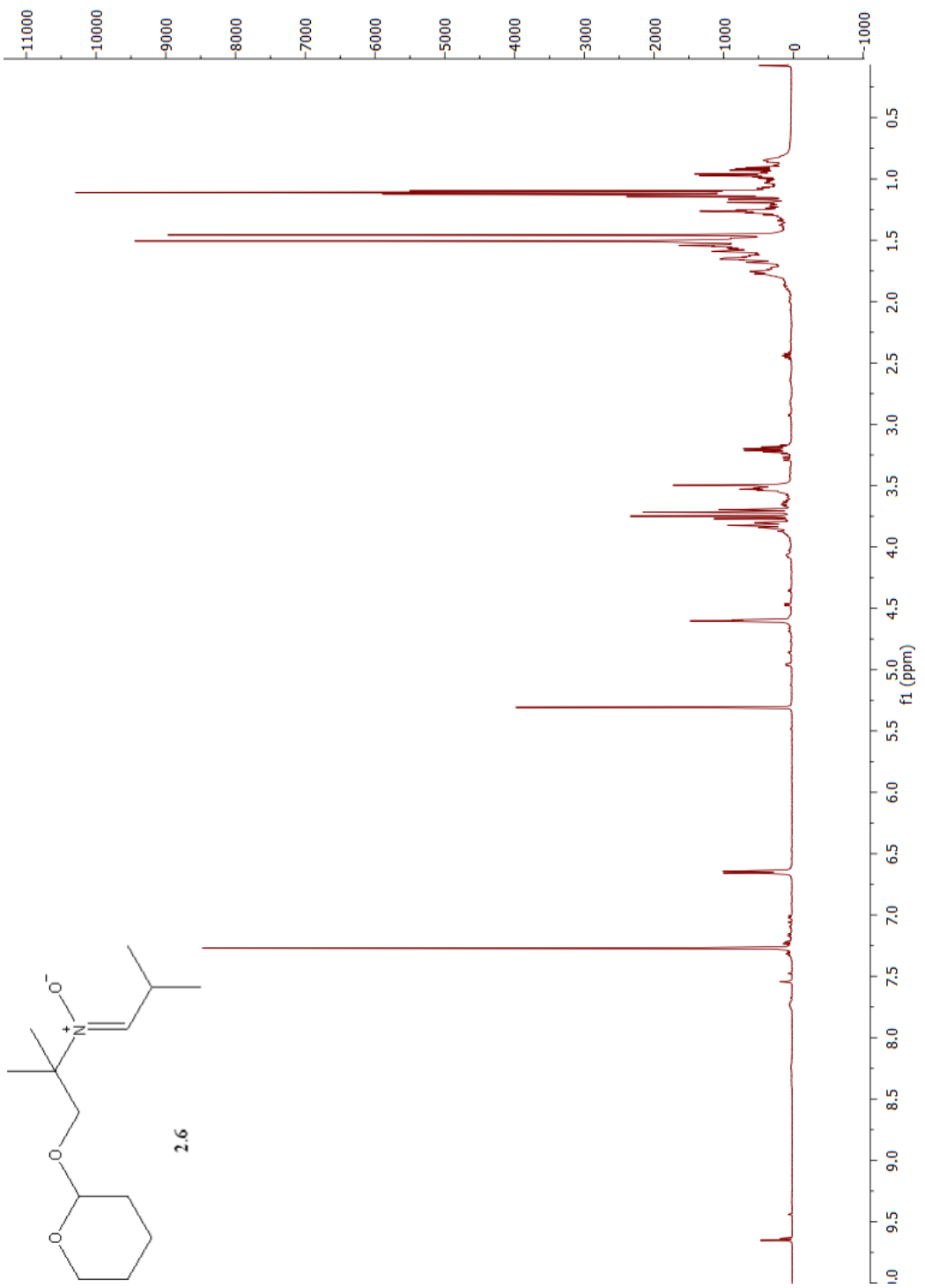
11000
10000
9000
8000
7000
6000
5000
4000
3000
2000
1000
0
-1000
0.5
1.0
1.5
2.0
2.5
3.0
3.5
4.0
4.5
5.0
5.5
6.0
6.5
7.0
7.5
8.0
8.5
9.0
9.5
f1 (ppm)
O
N
O
O
O

2.6

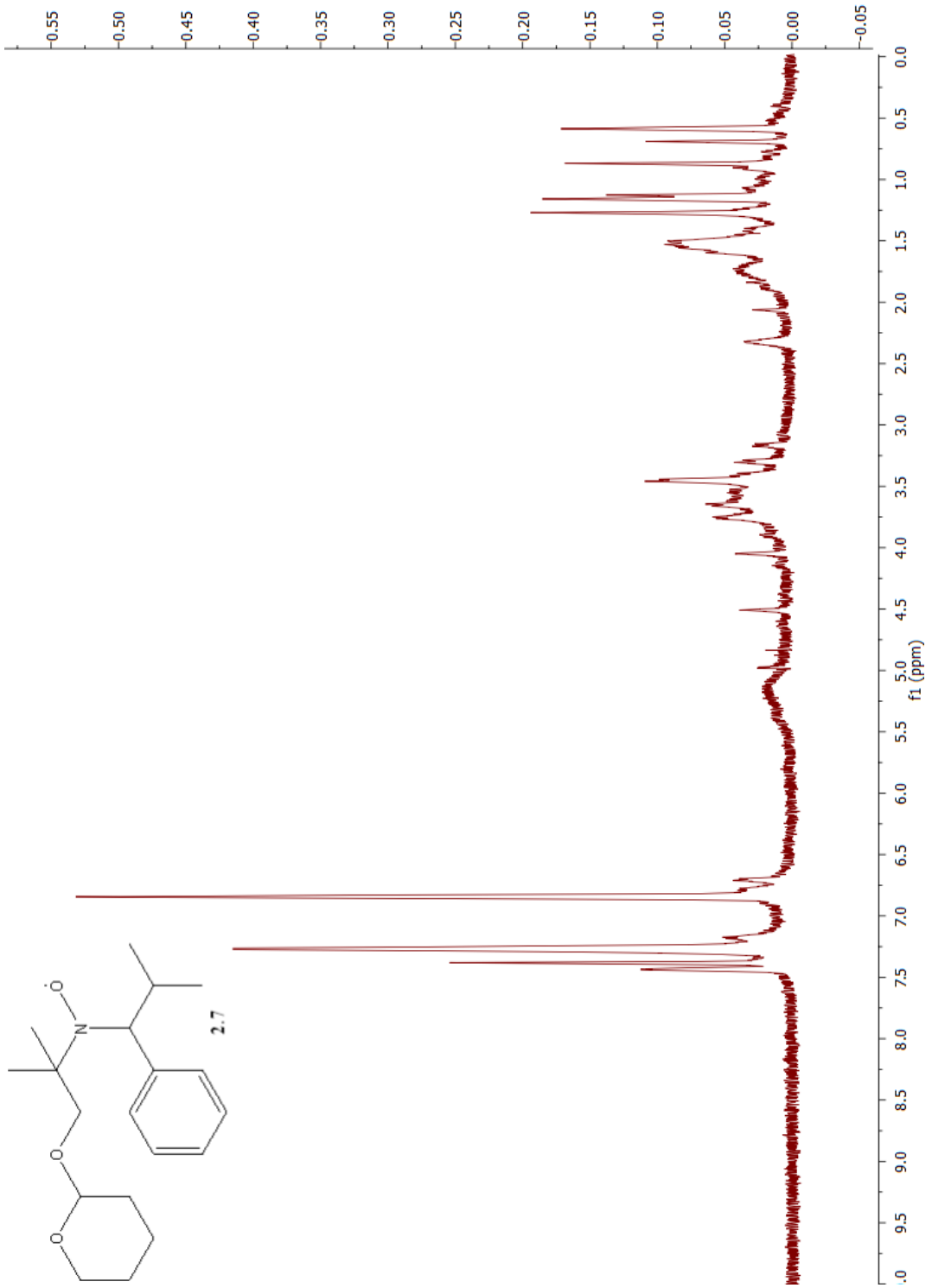
2.7
f1 (ppm)

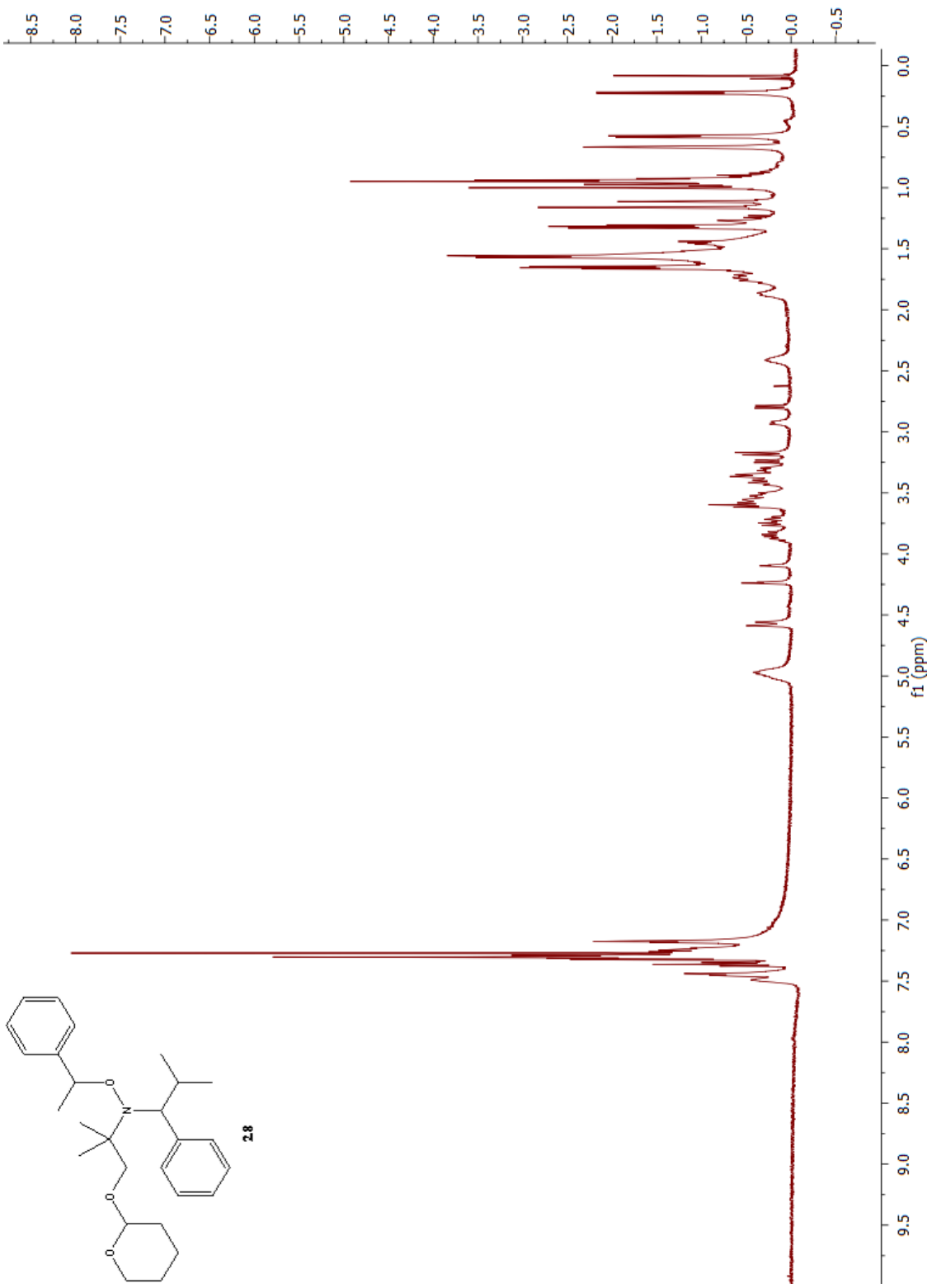
2.8
f1 (ppm)

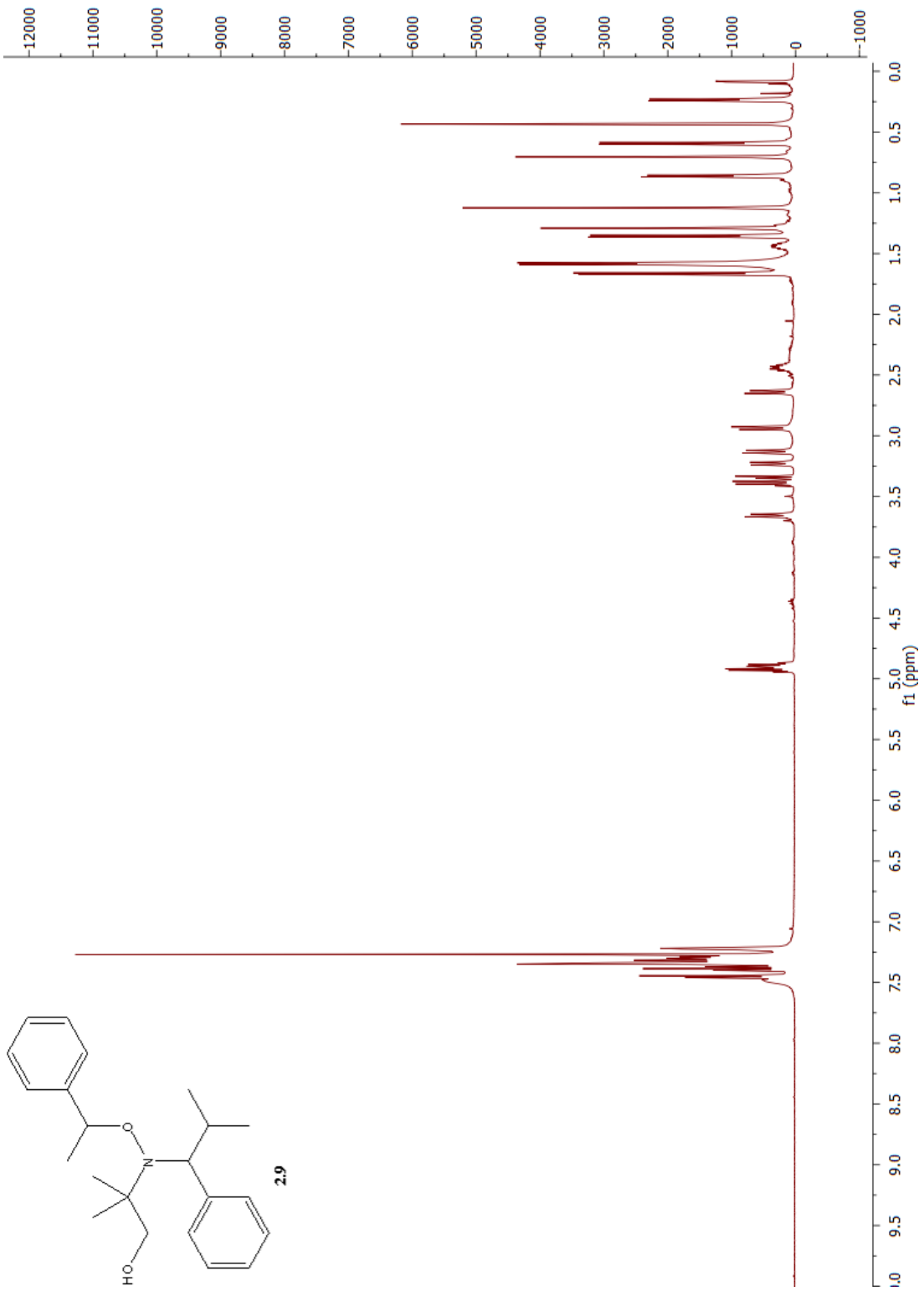
12000
11000
10000
9000
8000
7000
6000
5000
4000
3000
2000
1000
0
-1000
0.0
0.5
1.0
1.5
2.0
2.5
3.0
3.5
4.0
4.5
5.0
5.5
6.0
6.5
7.0
7.5
8.0
8.5
9.0
9.5
f1 (ppm)
HO
O
N
2.9

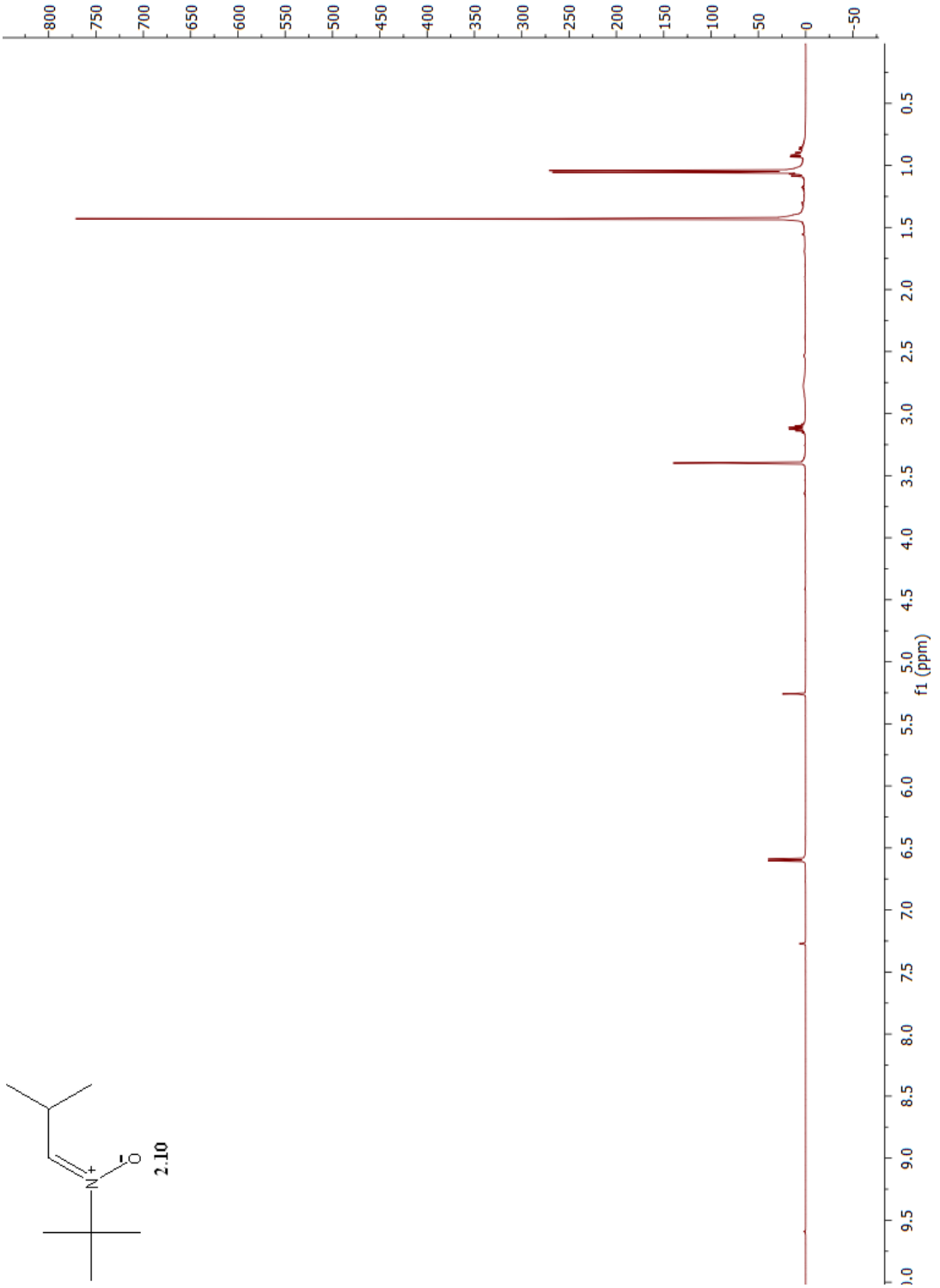

2.10

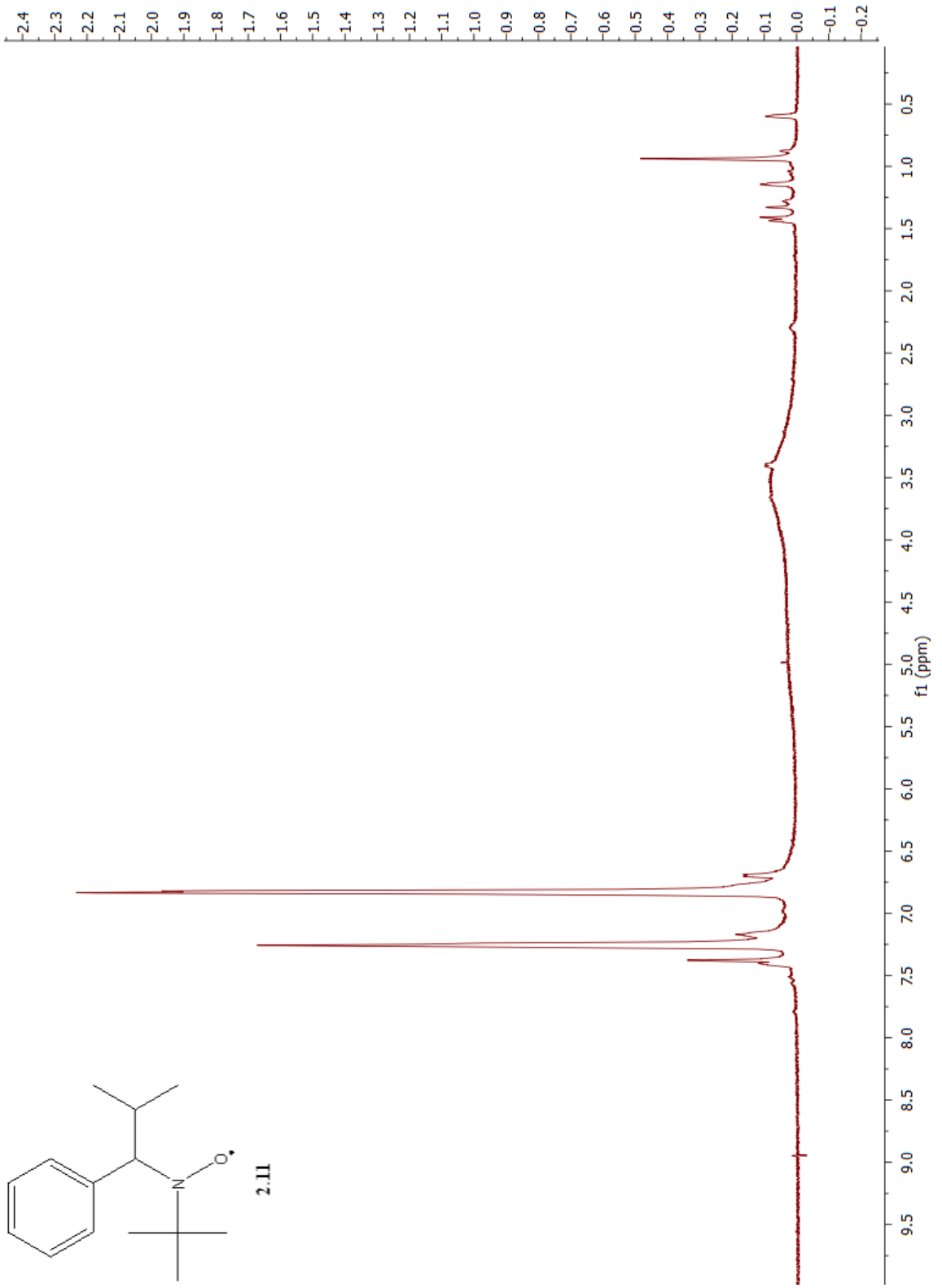

2.11

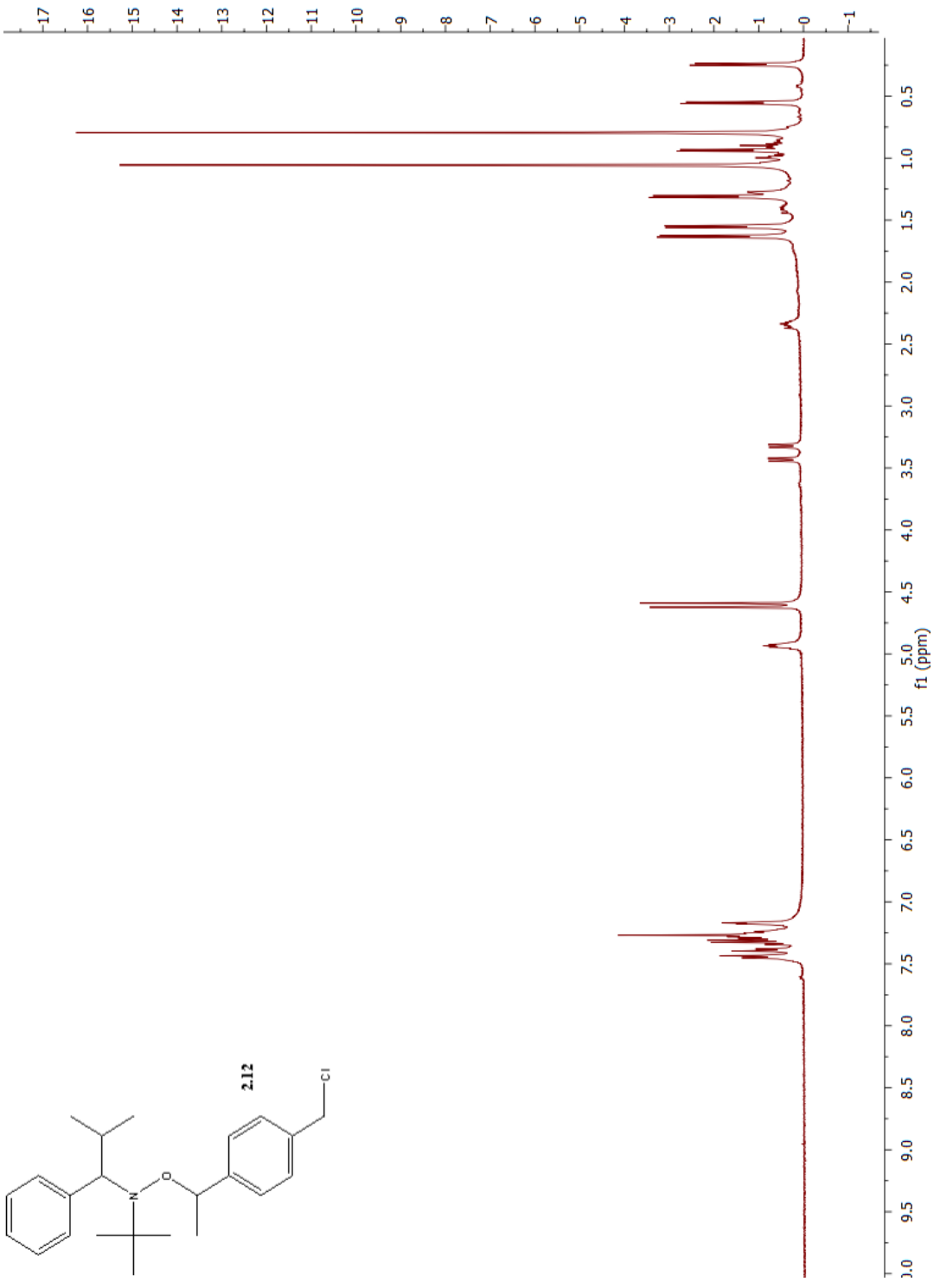
2.12
Cl
N
O
f1 (ppm)

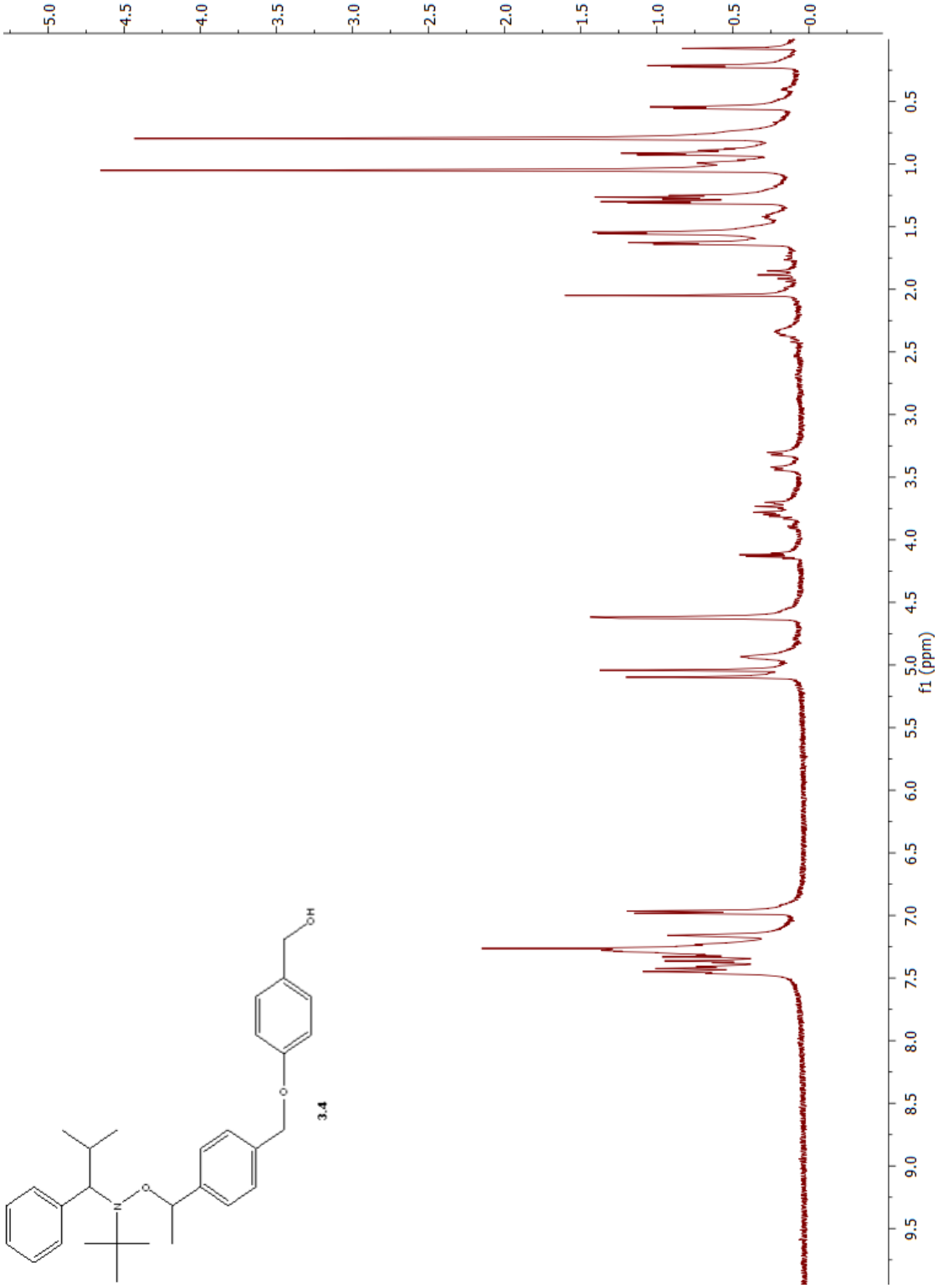
3.4
f1 (ppm)

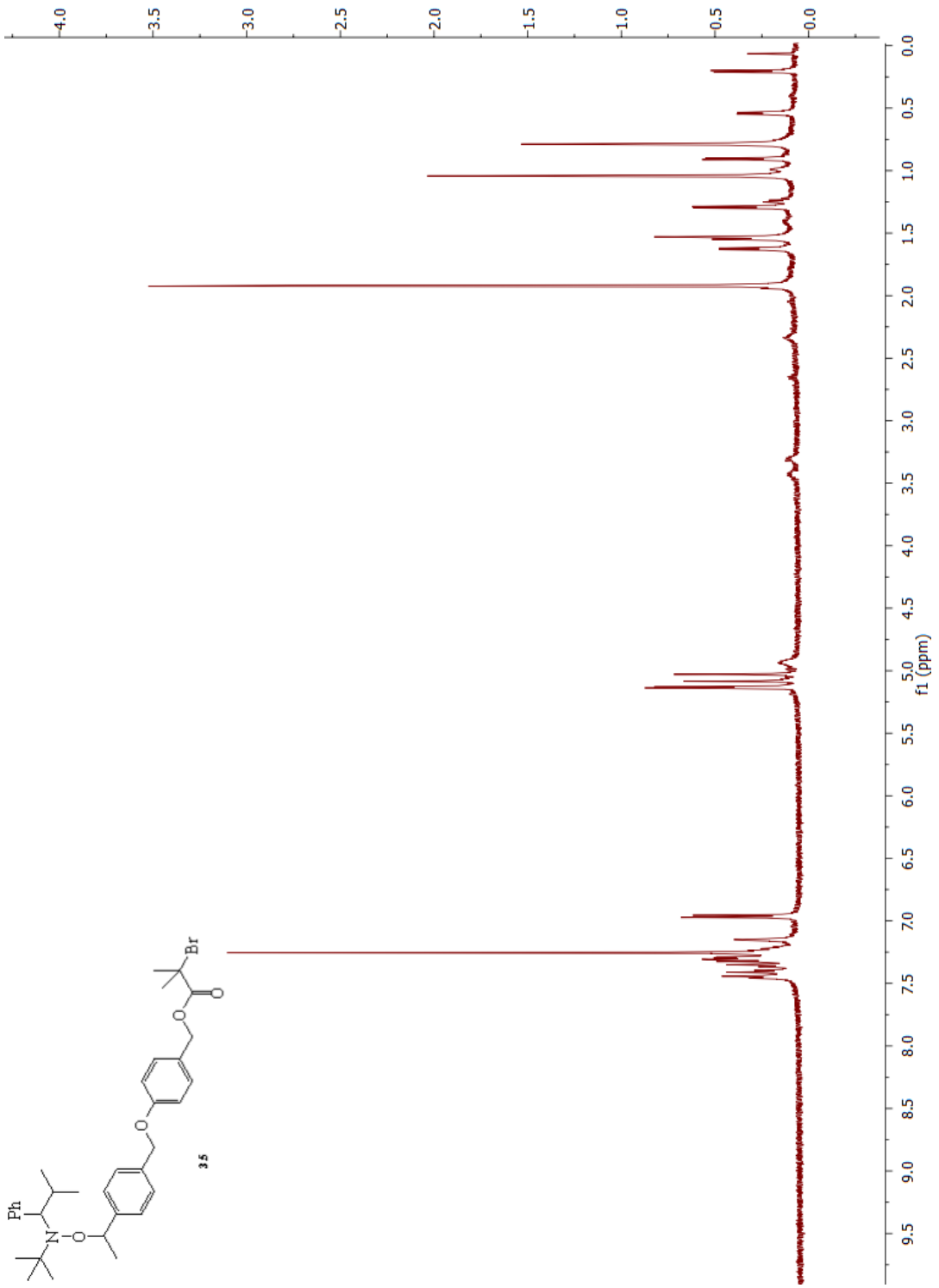
Ph
N
O
O
O
O
Br
O
3.5
f1 (ppm)

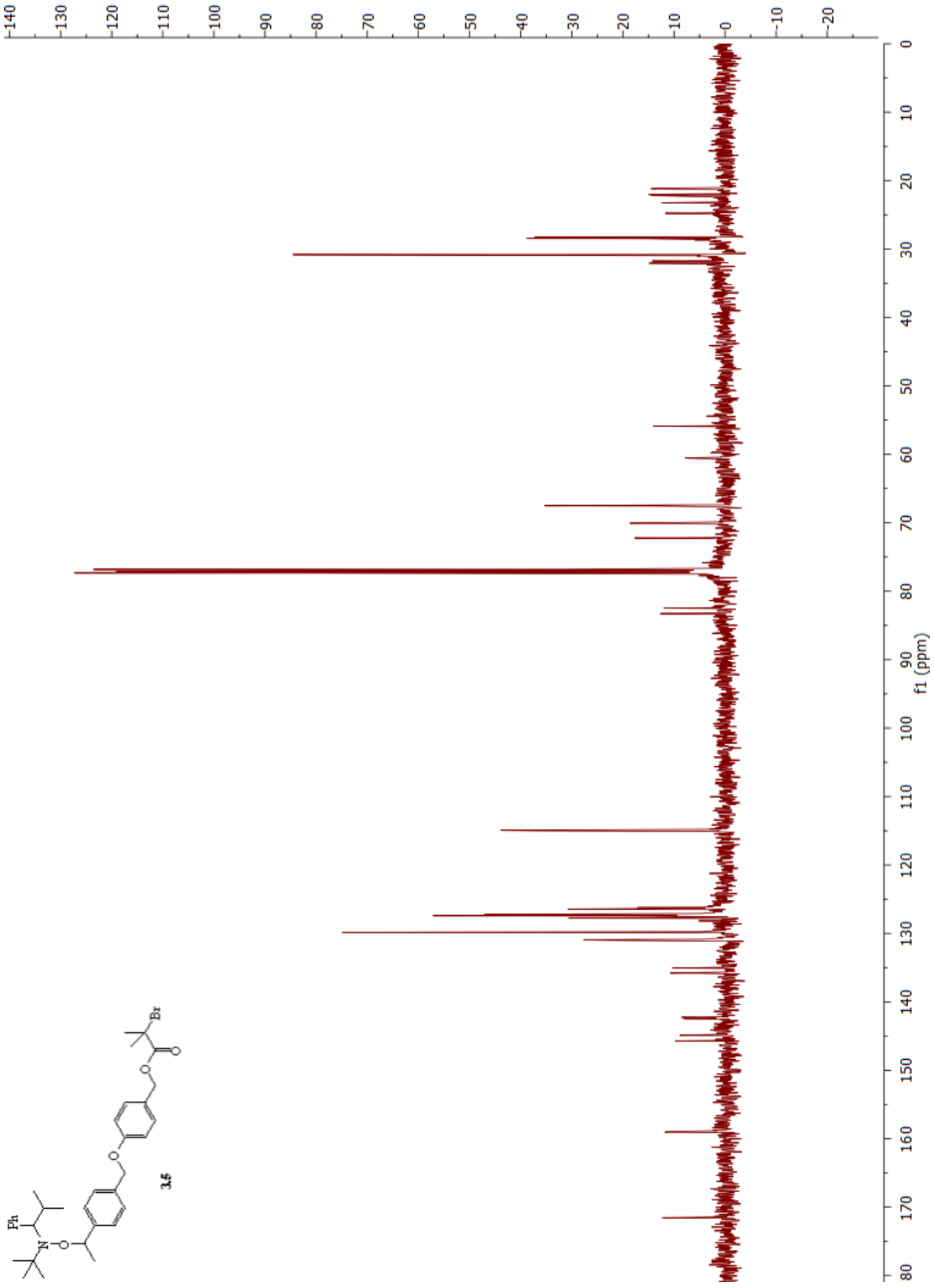
Ph
N
O
O
O
O
O
Br
3.5
f1 (ppm)

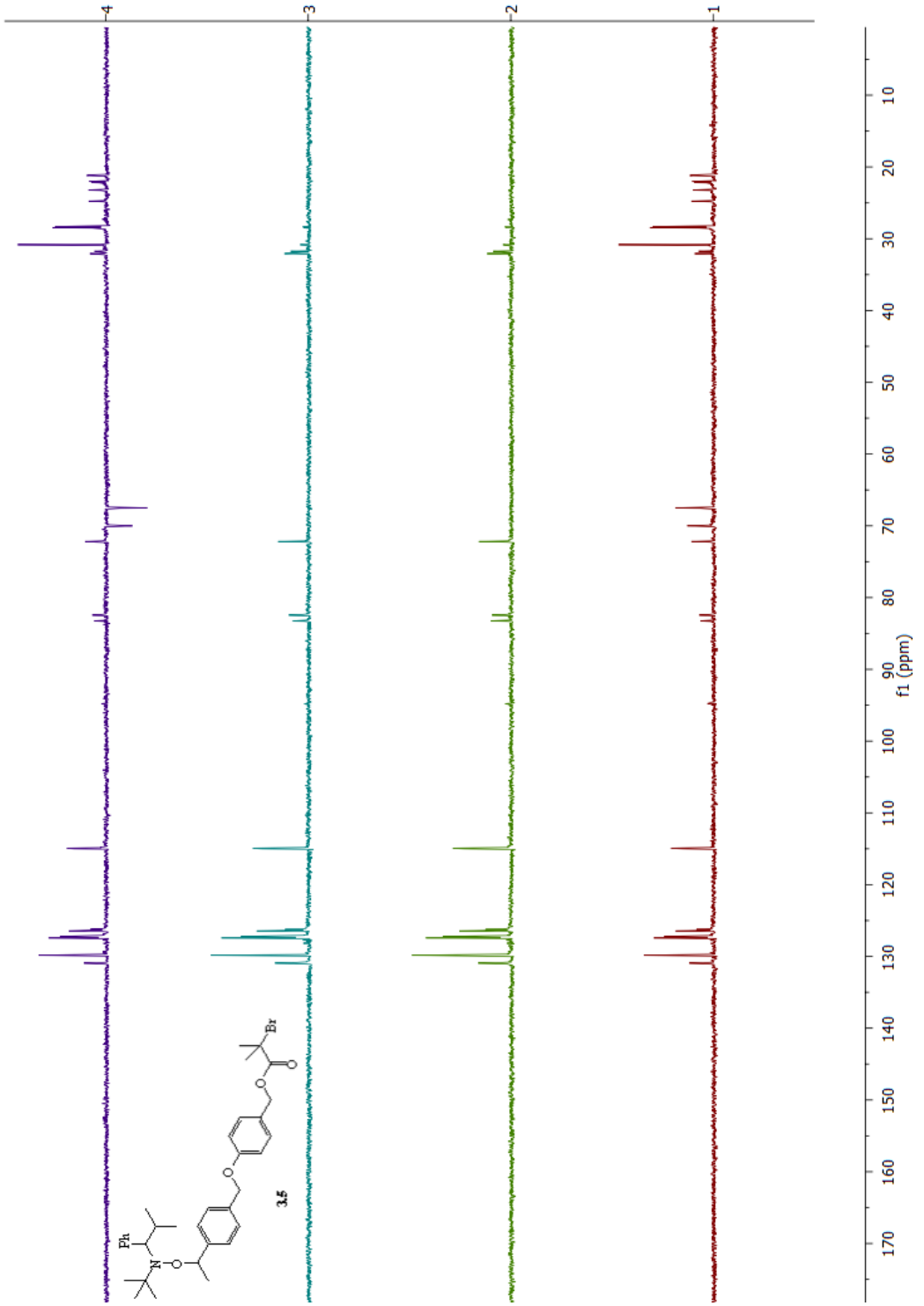
4
3
2
1
Ph
N
O
O
O
O
Br
O
3.5
10
20
30
40
50
60
70
80
90
100
110
120
130
140
150
160
170
f1 (ppm)

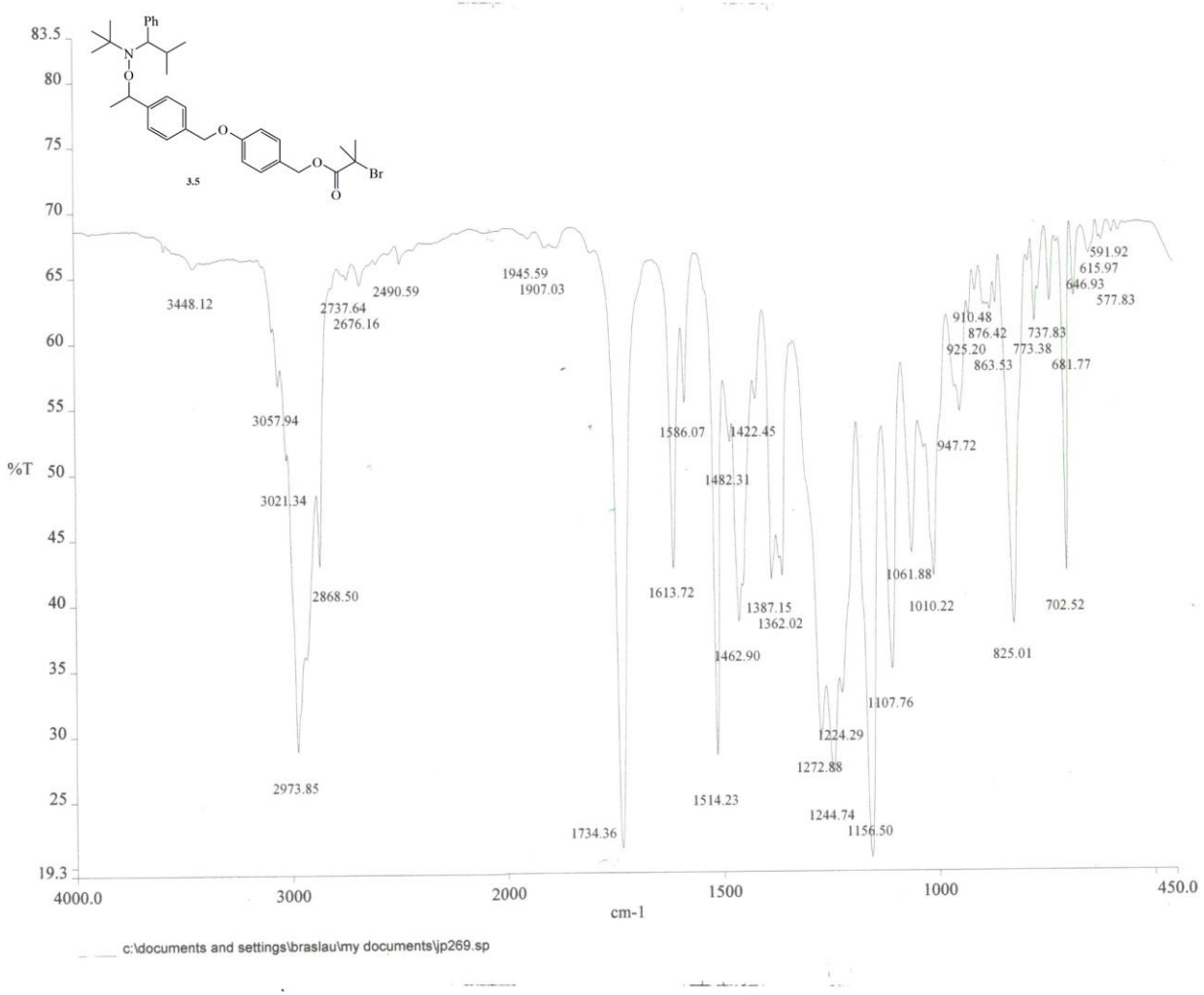
3.5
%T
cm-1
3448.12
3057.94
3021.34
2973.85
2868.50
2737.64
2676.16
2490.59
1945.59
1907.03
1734.36
1613.72
1586.07
1514.23
1482.31
1462.90
1422.45
1387.15
1362.02
1272.88
1244.74
1224.29
1156.50
1107.76
1061.88
1010.22
947.72
925.20
910.48
876.42
863.53
825.01
773.38
737.83
702.52
681.77
646.93
615.97
591.92
577.83
c:\documents and settings\braslau\my documents\jp269.sp

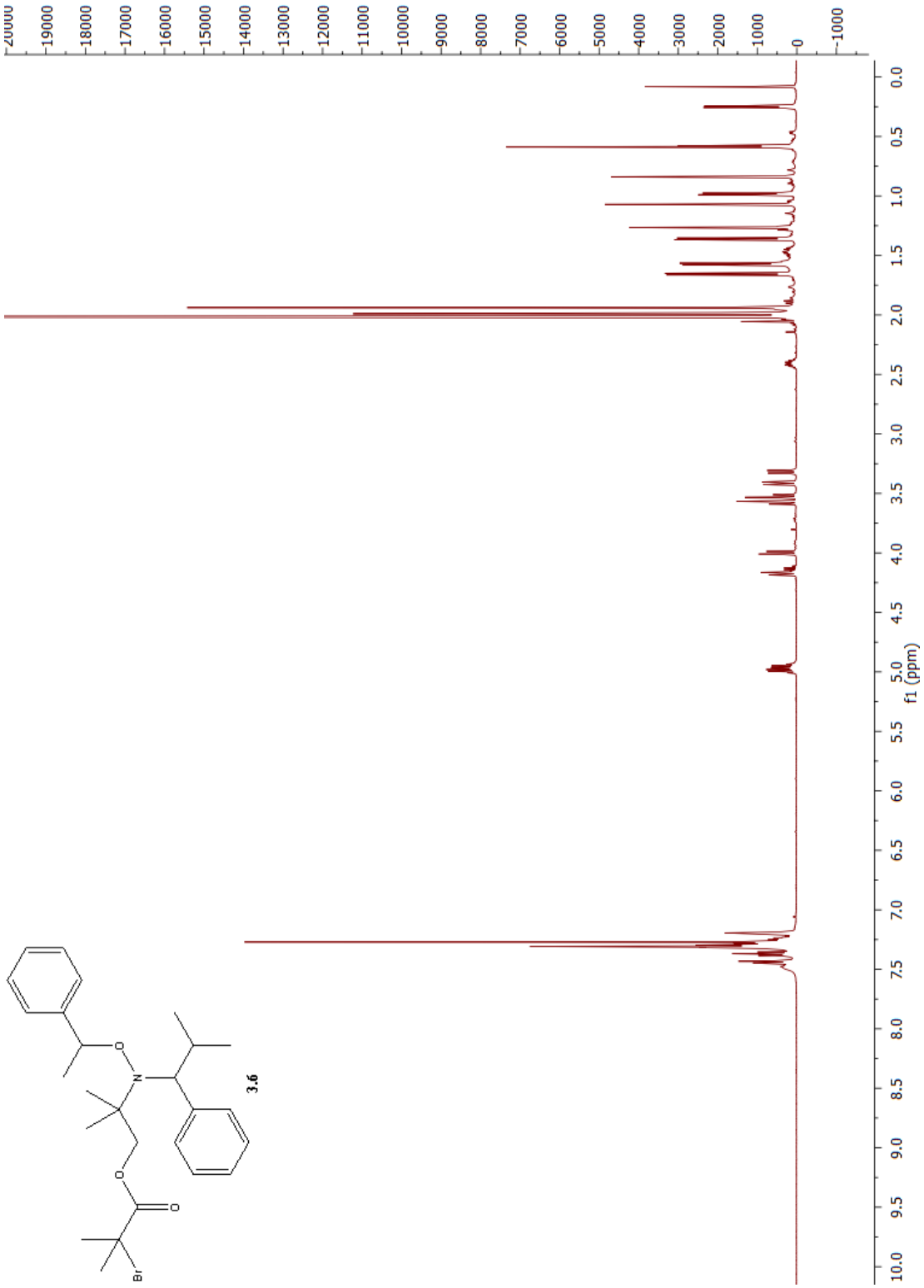
3.6
f1 (ppm)

Bibliography

1. http://www.novasterilis.com/index.php/application/supercritical-co2 (accessed Mar 21, 2017).

2. Alaimo, D.; Beigbeder, A.; Dubois, P.; Broze, G.; Jérôme, C.; Grignard, B. *Polym. Chem.* **2014**, *5* (18), 5273.

3. Aldabbagh, F.; Zetterlund, P. B.; Okubo, M. *Macromolecules* **2008**, *41* (7), 2732.

4. Aldabbagh, F.; Zetterlund, P. B.; Okubo, M. *Eur. Polym. J.* **2008**, *44* (12), 4037.

5. Barner-Kowollik, C.; Buback, M.; Charleux, B.; Coote, M. L.; Drache, M.; Fukuda, T.; Goto, A.; Klumperman, B.; Lowe, A. B.; Mcleary, J. B.; Moad, G.; Monteiro, M. J.; Sanderson, R. D.; Tonge, M. P.; Vana, P. *J. Polym. Sci. Part A: Polym. Chem.* **2006**, *44* (20), 5809.

6. Benoit, D.; Chaplinski, V.; Braslau, R.; Hawker, C. J. *J. Am. Chem. Soc.* **1999**, *121* (16), 3904.

7. Canelas, D. A.; DeSimone, J. M. *Macromolecules* **1997**, *30* (19), 5673.

8. Couvreur, L.; Lefay, C.; Belleney, J.; Charleux, B.; Guerret, O.; Magnet, S. *Macromolecules* **2003**, *36* (22), 8260.

9. Crich, D.; Grant, D.; Bowers, A. A. *J. Am. Chem. Soc.* **2007**, *129* (40), 12106.

10. Dao, J.; Benoit, D.; Hawker, C. J. *J. Polym. Sci., Part A: Polym. Chem.* **1998**, *36* (12), 2161.

11. Darling, T. R.; Davis, T. P.; Fryd, M.; Gridnev, A. A.; Haddleton, D. M.; Ittel, S. D.; Matheson, R. R.; Moad, G.; Rizzardo, E. *J. Polym. Sci., Part A: Polym. Chem.* **2000**, *38* (10), 1706.

12. DeSimone, J. M.; Maury, E. E.; Menceloglu, Y. Z.; McClain, J. B.; Romack, T. J.; Combes, J. R. *Science* **1994**, *265* (5170), 356.

13. Dornow, A.; Müller, A. *Chem. Ber.* **1960**, *93* (1), 41.

14. Fischer, H. *J. Am. Chem. Soc.* **1986**, *108* (14), 3925.

15. Georges, M. K.; Veregin, R. P. N.; Kazmaier, P. M.; Hamer, G. K. *Macromolecules* **1993**, *26* (11), 2987.

16. Grignard, B.; Jérôme, C.; Calberg, C.; Jérôme, R.; Wang, W.; Howdle, S. M.; Detrembleur, C. *Chem. Commun.* **2008**, 314.

17. Grignard, B.; Jérôme, C.; Calberg, C.; Jérôme, R.; Detrembleur, C. *Eur. Polym. J.* **2008**, 861.

18. Hawker, C. J. *J. Am. Chem. Soc.* **1994**, *116* (24), 11185.

19. Hill, N. L.; Braslau, R. *J. Polym. Sci., Part A: Polym. Chem.* **2007**, *45* (11), 2341.

20. Hyatt, J. A. *J. Org. Chem.* **1984**, *49* (26), 5097.

21. Kamigaito, M.; Ando, T.; Sawamoto, M. *Chem. Rev.* **2001**, *101* (12), 3689.

22. Kawaguchi, S.; Ito, K. In *Polymer Particles*; Okubo, M., Ed.; Springer: Berlin and Heidelberg, 2005; Vol. 175, pp 299–328.

23. Kendall, J. L.; Canelas, D. A.; Young, J. L.; DeSimone, J. M. *Chem. Rev.* **1999**, *99* (2), 543.

24. Lacroix-Desmazes, P.; Andre, P.; Desimone, J. M.; Ruzette, A.-V.; Boutevin, B. *J. Polym. Sci., Part A: Polym. Chem.* **2004**, *42* (14), 3537.

25. Magee, C.; Earla, A.; Petraitis, J.; Higa, C.; Braslau, R.; Zetterlund, P. B.; Aldabbagh, F. *Polym. Chem.* **2014**, *5* (19), 5725.

26. Marque, S.; Le Mercier, C.; Tordo, P.; Fischer, H. *Macromolecules* **2000**, 33 (12), 4403.

27. Matyjaszewski, K.; Gaynor, S.; Greszta, D.; Mardare, D.; Shigemoto, T. *J. Phys. Org. Chem.* **1995**, *8* (4), 306.

28. Matyjaszewski, K.; Xia, J. *Chem. Rev.* **2001**, *101* (9), 2921.

29. McHale, R.; Aldabbagh, F.; Zetterlund, P. B.; Okubo, M. *Macromol. Rapid Commun.* **2006**, *27* (17), 1465.

30. McHale, R.; Aldabbagh, F.; Zetterlund, P. B.; Okubo, M. *Macromol. Chem. Phys.* **2007**, *208* (16), 1813.

31. Moad, G.; Rizzardo, E.; Thang, S. H. *Aust. J. Chem.* **2006**, *59* (10), 669.

32. Nilsen, A.; Braslau, R. *J. Polym. Sci., Part A: Polym. Chem.* **2006**, *44* (2), 697.

33. O'Brien, G.; Ph.D. Dissertation, University of California, Santa Cruz, **2007**, p. 149.

34. O'Connor, P.; Zetterlund, P. B.; Aldabbagh, F. *Macromolecules* **2010**, *43* (2), 914.

35. Otsu, T.; Yoshida, M.; Tazaki, T. *Macromol. Rapid Commun.* **1982**, *3* (2), 133.

36. Rindfleisch, F.; DiNoia, T. P.; McHugh, M. A. *J. Phys. Chem.* **1996**, *100* (38), 15581.

37. Rindfleisch, F.; DiNoia, T.; McHugh, M. *Polym. Mater. Sci. Eng.* **1996**, *74*, 178.

38. Ruehl, J.; Braslau, R. *J. Polym. Sci., Part A: Polym. Chem.* **2007**, *45* (10), 2015.

39. Ryan, J.; Aldabbagh, F.; Zetterlund, P. B.; Okubo, M. *Polymer* **2005**, *46* (23), 9769.

40. Shipp, D. A. *J. Macromol. Sci. C.* **2005**, *45* (2), 171.

41. Sobek, J.; Martschke, R.; Fischer, H. *J. Am. Chem. Soc.* **2001**, *123* (12), 2849.

42. Span, R.; Wagner, W. *J. Phys. Chem. Ref. Data* **1996**, *25* (6), 1509.

43. Thurecht, K. J.; Howdle, S. M. *Aust. J. Chem.* **2009**, *62* (8), 786

44. Valtola, L.; Koponen, A.; Karesoja, M.; Hietala, S.; Laukkanen, A.; Tenhu, H.; Denifl, P. *Polymer* **2009**, *50* (14), 3103.

45. Villarroya, S.; Zhou, J.; Thurecht, K. J.; Howdle, S. M. *Macromolecules* **2006**, *39* (26), 9080.

46. Xia, J.; Johnson, T.; Gaynor, S. G.; Matyjaszewski, K.; DeSimone, J. *Macromolecules* **1999**, *32* (15), 4802.

47. Zetterlund, P. B.; Aldabbagh, F.; Okubo, M. *J. Polym. Sci., Part A: Polym. Chem.* **2009**, *47* (15), 3711.

48. Zetterlund, P. B. *Macromol. Theory Simul.* **2010**, *19*, 11.